ACS OMEGA

http://pubs.acs.org/journal/acsodf

Article

Study on Adsorption Characteristics of Deep Coking Coal Based on Molecular Simulation and Experiments

Zhaofeng Wang, Shasha Si,* Yongjie Cui, Juhua Dai, and Jiwei Yue

Cite This: *ACS Omega* 2023, 8, 3129−3147

Read Online

ACCESS | Metrics & More | Article Recommendations

ABSTRACT: To study the effect of high temperature and high pressure on the adsorption characteristics of coking coal, Liulin coking coal and Pingdingshan coking coal were selected as the research objects, and isotherm adsorption curves at different temperatures and pressures were obtained by combining isotherm adsorption experiments and molecular dynamics methods. The effect of high temperature and high pressure on the adsorption characteristics of coking coal was analyzed, and an isothermal adsorption model suitable for high-temperature and high-pressure conditions was studied. The results show that the adsorption characteristics of deep coking coal can be well characterized by the molecular dynamics method. Under a supercritical condition, the excess adsorption capacity of methane decreases with the increase of temperature. With the increase of pressure, the excess adsorption capacity rapidly increases in the early stage, temporarily stabilizes in the middle stage, and decreases in the later stage. Based on the classical adsorption model, the adsorption capacity of coking coal under high-temperature and high-pressure environments is fitted. The fitting degree ranges from good to poor. The order is D−R > D−A > L−F >BET > Langmuir, and combined with temperature gradient, pressure gradient, and the D−R adsorption model, it can be seen that after 800 m deep in Liulin Mine and 400 m deep in Pingdingshan Mine, the adsorption capacity of coking coal to methane decreases with the increase of depth.

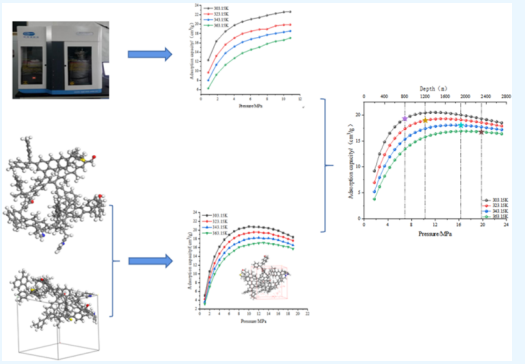

1. INTRODUCTION

The development and utilization of coking coal plays a vital role in the development of China's coal industry and is an indispensable resource for China's economic construction.[1] In recent years, with the increase in mining depth, the environmental conditions of high ground temperature and high gas pressure have appeared in the storage of coal.[2,3] Coking coal mines that originally belonged to the low-gas category have been upgraded to high-gas or even outburst mines. For a long time, the focus of gas control has mainly been on highly metamorphic coal represented by anthracite, and there are few studies on coking coal. In particular, lack of research on the gas adsorption characteristics of coking coal under high-temperature and high-pressure conditions seriously restricts the development of coalbed methane, gas disaster control, and safe mining in coking coal mining areas.[4−6] Therefore, it is necessary to study the adsorption characteristics of coking coal on methane under high-temperature and high-pressure environments.

Many scholars have performed much research on the methane adsorption characteristics of coal through laboratory tests, theoretical analyses, and numerical simulations. In these experimental tests, the main focus has been on the effect of constant temperature and constant pressure, especially single-factor temperature and pressure, on the gas adsorption characteristics.[7,8] Levy, Bustin, Sakurovs et al.[9−11] found that the adsorption amount of gas on the coal surface increased with increasing pressure and decreased with increasing temperature. Zhaofeng et al.[12] studied the adsorption/desorption characteristics of anthracite from 244.15 to 304.15 K and found that the lower the temperature, the greater the gas adsorption capacity of coal. When the temperature is constant, the methane adsorption capacity increases with increasing gas pressure, but there is a limit to the gas adsorption capacity for a certain quality coal sample. Liu Gaofeng[13] tested the gas adsorption capacity of anthracite at a pressure of 0−10 MPa and found that the rate of change of the adsorption capacity showed a rapid decrease in the early stage, a slow decrease in the middle stage, and a stable later stage as the pressure increased. Zhang[14] conducted adsorption experiments on dry anthracite coal samples with different particle sizes and anthracite coal samples with equilibrium water and

Received: October 12, 2022
Accepted: December 23, 2022
Published: January 10, 2023

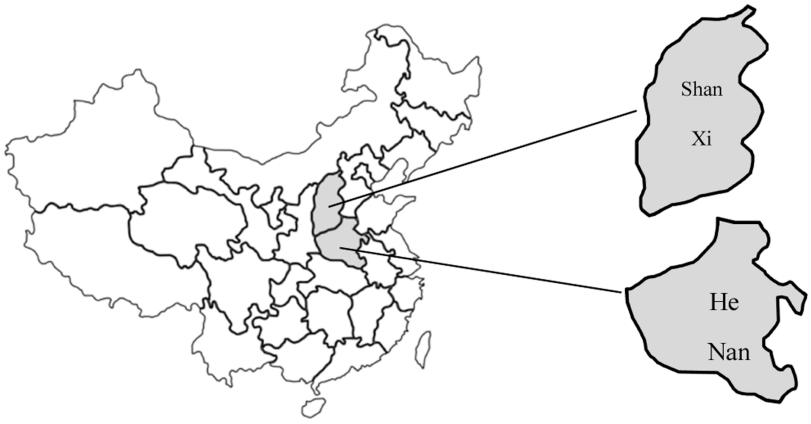

Figure 1. Sampling location map.

found that with increasing pressure, the adsorption capacity did not always increase, but when the pressure reached a certain value, the adsorption capacity decreased instead. With an increase in the coal seam mining depth, the temperature and pressure of the coal seam will increase significantly, which together affect the gas adsorption characteristics of coal, thus restricting the development of deep coalbed methane, gas disaster control, and safe mining. Therefore, it is of great significance to study the combined effect of temperature and pressure on the adsorption of methane by coking coal.

Coal is a complex porous medium, and the adsorption of gas on the pore surface is mainly physical adsorption.[15] Many scholars have conducted research on this issue and proposed a series of adsorption models. The commonly used adsorption models include the Langmuir adsorption model based on single-molecule adsorption theory, the Langmuir−Freundlich (L−F) adsorption model and the BET adsorption model based on bilayer adsorption theory, and the Dubin−Radushkevich (D−R) and Dubin−Astakhov (D−A) adsorption models based on adsorption potential theory.[16] Pan et al.[17] studied the adsorption relationship between coal and methane with different degrees of metamorphism at different temperatures and pressures and found that coal with different degrees of metamorphism showed different adsorption capacities and adsorption isotherms. Divó-Matos[18] studied the isotherm adsorption model of high-pressure gas and found that the adsorption isotherm model derived from the Redlich−Kwong equation can better characterize the adsorption behavior under a high-pressure environment. Xie[19] studied the methane adsorption characteristics in the range of 253.15−293.15 K and found that the adsorption model based on the adsorption potential theory could well characterize the methane adsorption behavior; Lu et al.[20] studied the methane adsorption characteristics of tectonic coal in the Huaibei coalfield and found that coals with different metamorphic degrees have different suitabilities for the same adsorption model; Dengand others[21] studied the methane adsorption heat of coal and found that the D−A adsorption model has the best fitting effect in the low-pressure range; Hou et al.[22] studied the change of the adsorption force of high-temperature and high-pressure gas on the coal surface and found that under the action of high temperature and high pressure, the Langmuir equation can still be used to accurately describe the gas adsorption process of coal. Whether the traditional model or the deduced adsorption model can well characterize the adsorption characteristics of coking coal under the joint influence of high temperature and high pressure is still controversial and has considerable room for development. Therefore, it is of great significance to find an adsorption model considering both temperature and pressure.

The most fundamental reason for the change in the macroscopic properties of coal is the change in its microstructure. Therefore, many scholars have explored the adsorption characteristics of coal for methane from a microscopic perspective.[23−25] Hu[26] studied the adsorption and diffusion of methane and other small molecular gases on coal by molecular simulation and found that the adsorption isotherm obtained by molecular simulation was similar to the experimental results. Khaddour[27] studied the adsorption of pure methane in activated carbon by combining classical canonical integrated Monte Carlo molecular simulation and gravimetric-based isotherm adsorption experiments and found that the combination of the two can completely characterize the activated carbon substrate and its methane storage capacity. Song[28] simulated the adsorption of methane by coal molecules and compared it with the adsorption of methane on graphene and found that the adsorption of methane by macromolecular vitrinites mainly depends on the adsorption site, adsorption site orientation, and adsorption orientation. Both the data and the adsorption data are in good agreement with the Langmuir and DA isotherm adsorption models. The above research shows that molecular simulation has an important theoretical value for gas adsorption research, and the combination of experiments and molecular simulation can better characterize the adsorption behavior of coal.

In summary, to study the adsorption characteristics of coking coal under high-temperature and high-pressure conditions, a typical coal macromolecular model was established and optimized by molecular simulation software, and the optimized model with the lowest energy was selected to simulate adsorption isotherms under different temperature conditions. Methane adsorption was measured and corrected by isothermal experiments. The isothermal adsorption model suitable for high temperature and high pressure was obtained by comparing the commonly used adsorption models. Through the combination of molecular simulation and experimental methods, the methane adsorption characteristics of coking coal are quantitatively analyzed, the influence of high temperature and high pressure on the methane adsorption of coking coal is revealed, and the methane adsorption capacity of coal seams at different depths is predicted, which provides a theoretical basis for the safe mining of deep coal seams in

https://doi.org/10.1021/acsomega.2c06593
ACS Omega 2023, 8, 3129−3147

Table 1. Basic Parameters of Coal Sample.....

numbering	TRD (g/cm^3)	ARD (g/cm^3)	Φ (%)	f	industrial analysis of coal		
					Mad (%)	Aad (%)	Vdaf (%)
LX	1.42	1.39	5.67	0.94	1.03	8.09	16.98
PS	1.38	1.35	8.03	0.84	0.49	18.25	24.91

Table 2. Coking Coal Molecular Simulation Parameters

options	method	optimize quality items	adsorbate	start pressure (kPa)	end pressure	position	load	balance steps	total number of steps in the process	temperature (K)
LX	metropolis	customized	CH_4	10	20,000 kPa	COMPASS	forcefield assigned	100,000	10,00,000	303.15 323.15 343.15 363.15
PS	metropolis	customized	CH_4	10	20,000 kPa	COMPASS	forcefield assigned	100,000	10,00,000	303.15 323.15 343.15 363.15

coking coal mining areas and the prevention and control of gas disasters.

2. TEST

2.1. Collection and Preparation of Coal Samples. North China, East China, and Central South China are important coking coal production and reserve bases in China. The coking coal in Liulin, Shanxi, has low ash content and excellent quality and is a rare type of conventional coking coal. The Xingwu Coal Mine is located 6 km east of Liulin County, Shanxi Province, and the average thickness of the coal seam is 0.89 m. The Pingdingshan mining area of Henan Province is the main coking coal production base in central South China, with rich coking coal reserves. The Pingdingshan No. 12 Mine is located in the middle and west of the Pingdingshan coalfield of Henan Province and is a severely protruding mine. Based on adsorption isotherm experiments and molecular simulations, this paper explores the gas adsorption characteristics of deep coking coal in the above two main coking coal producing areas. The experiment selected the coal sample of the No. 8 coal seam in the middle section of the Taiyuan Formation in the Liulin Xingwu Mine (LX), Shanxi Province, and the average gas content of this coal seam was 14.98 m^3/t. The maximum original gas pressure of the coal seam is 1.2 MPa; Pingdingshan No. 12 Coal Mine (PS) Ji 15-31050 working face has a burial depth of 994 m, an average gas content of 15.256 m^3/t, and a maximum coal seam gas pressure of 2.15 MPa (Figure 1). The collected coal samples were pulverized and sieved with a particle size of less than 0.2 mm for basic parameter determination. The measurement results of the basic parameters of the experimental coal samples are given in Table 1.

Table 1 shows the *TRD* and *ARD* (the true density and apparent density) of coal, respectively. The true density refers to the density obtained by dividing the powder mass (W) by the volume, excluding the voids inside and outside the particles (true volume V_t). The mass per unit apparent area of an object is called apparent density.

Φ represents porosity. Porosity is the ratio of the pore volume of coal to the total volume of coal and can also be expressed by the pore volume (cm^3/g) contained in the unit mass of coal. Porosity is equal to (true density − apparent density)/(true density) × 100%.

M_{ad} is the water in coal; A_{ad} is the ash content in coal; and V_{ad} is the volatile matter in coal. These constitute the fundamental basis for understanding and mastering the nature of coal.

2.2. Test Plan. *2.2.1. Molecular Simulation Test Protocol.* Through Materials Studio molecular simulation software, coal macromolecular models based on Liulin Xingwu coking coal and Pingdingshan No. 12 coking coal were constructed, and their geometric optimization and annealing optimization were carried out. The coal macromolecular model with the lowest energy was selected for the construction of periodic boundary conditions. Isothermal adsorption simulations were carried out at different temperatures (303.15, 323.15, 343.15, 363.15 K) and the highest pressure of 20 MPa.

2.2.2. Isothermal Adsorption Simulation Scheme. The sorption module in Materials Studio was used to simulate the adsorption molecules. The simulation temperatures are 303.15, 323.15, 343.15, and 363.15 K, the gas pressure is in the range of 0−20 MPa, the adsorbent is the optimized coking coal stereomolecular model, and the adsorbate is methane gas molecules. A total of eight sets of simulation experiments were carried out. The parameter settings of the coking coal molecular simulation are shown in Table 2. When the number of simulated configurations reaches a certain numerical value and enters an equilibrium state, the simulation ends.

2.2.3. Experimental Scheme of Isothermal Adsorption. The experiment uses the Hsorb-2600 high-temperature and high-pressure gas adsorption instrument to carry out the isothermal adsorption experiment of coking coal under high-temperature and high-pressure conditions. The experimental equipment is shown in Figure 2.

The instrument can work in the temperature range of 77.15−873.15 K and the pressure range of 0.04−20 MPa and can choose the temperature and pressure for the coal to methane adsorption/desorption measurement experiment. In terms of temperature, pressure, accuracy, and other common

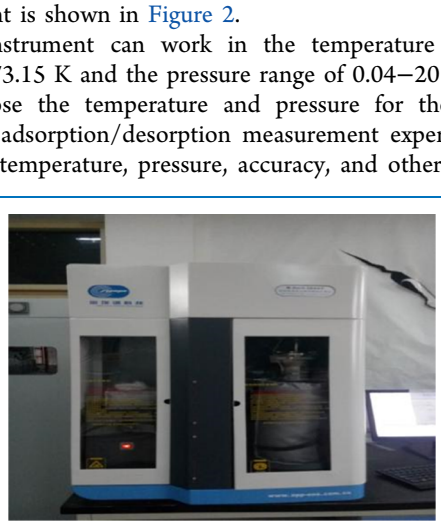

Figure 2. Hsorb-2600 high-temperature and high-pressure gas adsorbent instrument.

https://doi.org/10.1021/acsomega.2c06593
ACS Omega 2023, 8, 3129−3147

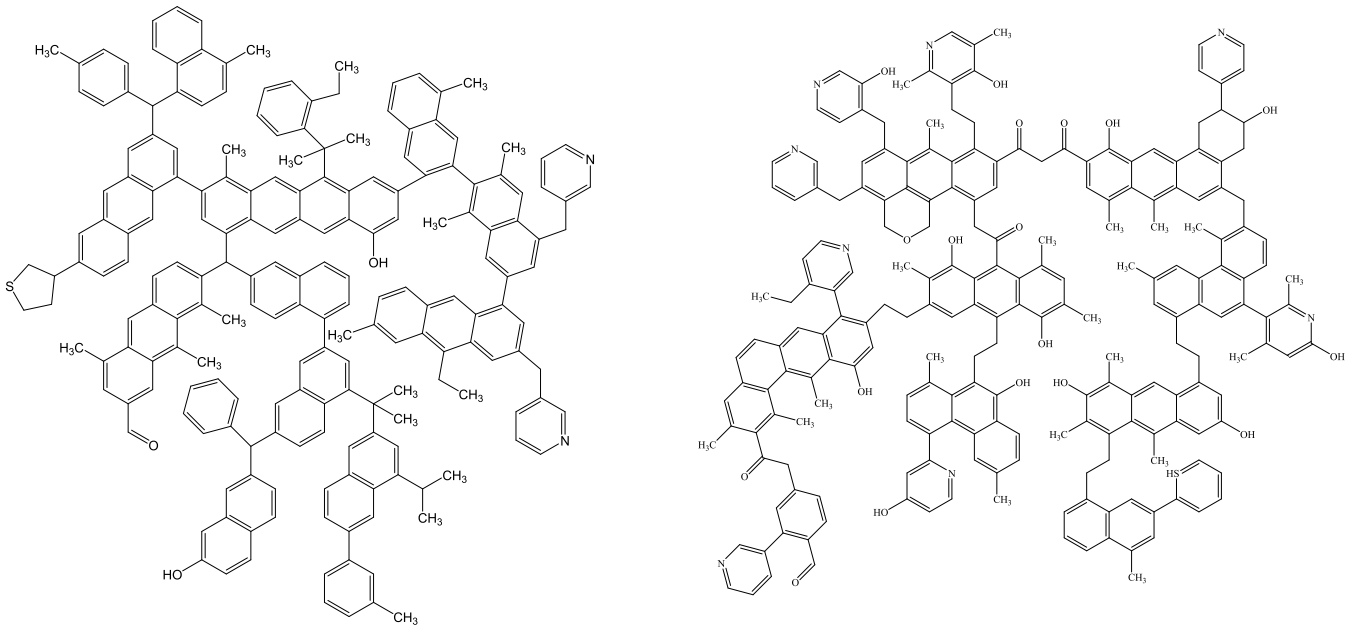

(a) Molecular structure of LX coal

(b) Molecular structure of PS coal

Figure 3. Macromolecular structure of coking coal.

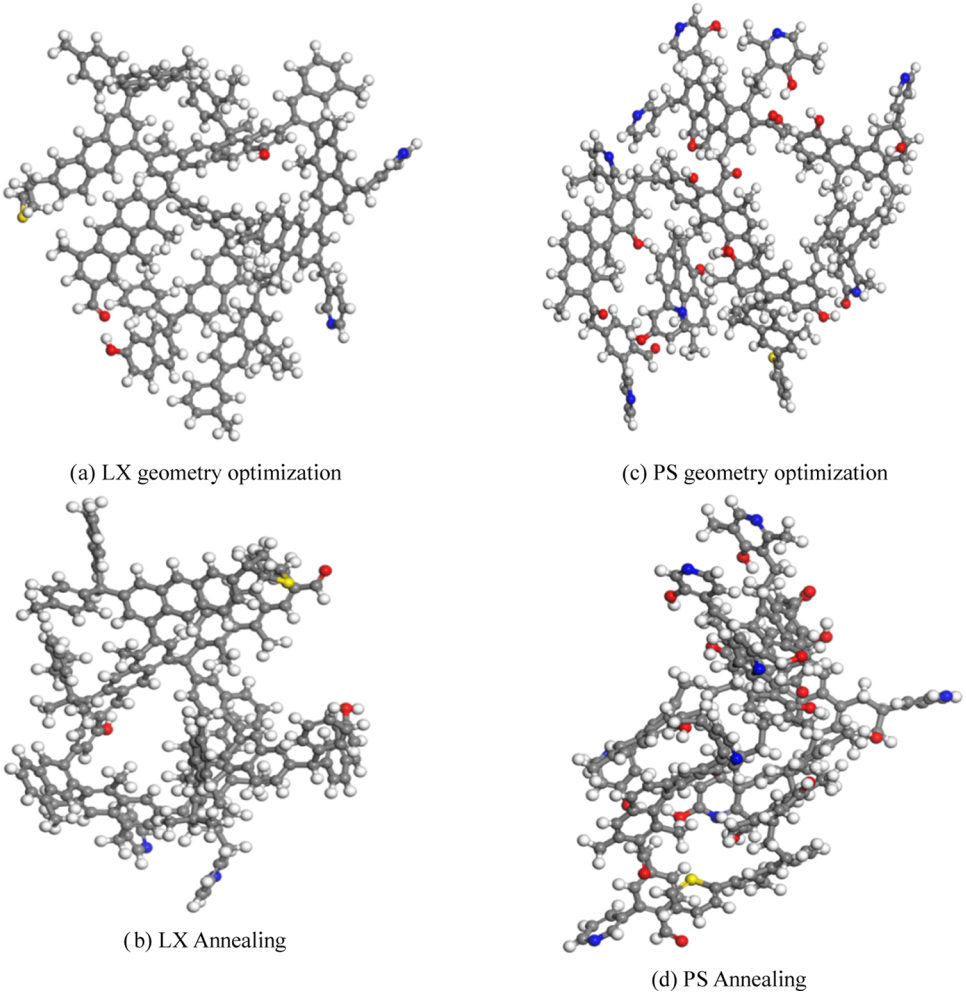

(a) LX geometry optimization

(c) PS geometry optimization

(b) LX Annealing

(d) PS Annealing

Figure 4. Energy-minimum conformation of the chemical structure model of the coking coal sample.

https://doi.org/10.1021/acsomega.2c06593
ACS Omega 2023, 8, 3129−3147

Table 3. Potential Energy Optimization Parameters of the LX Coking Coal Macromolecular Model

		E_V (kcal/mol)				E_N (kcal/mol)		
	E_{total} (kcal/mol)	E_B	E_A	E_T	E_I	E_{VAN}	E_E	E_H
initial structure	5446.33	1373.06	42.70	2194.82	100.87	684.28	634.62	0
final structure	2219.28	60.36	37.38	2171.88	60.109	130.97	−7.077	0

Table 4. Potential Energy Optimization Parameters of the PS Coking Coal Macromolecular Model

		E_V (kcal/mol)				E_N (kcal/mol)		
	E_{total} (kcal/mol)	E_B	E_A	E_T	E_I	E_{VAN}	E_E	E_H
initial structure	12140.51	3370.70	400.48	166.62	70.21	855.71	855.53	−0.18
final structure	1337.82	253.96	184.82	132.36	27.79	465.60	464.94	−0.66

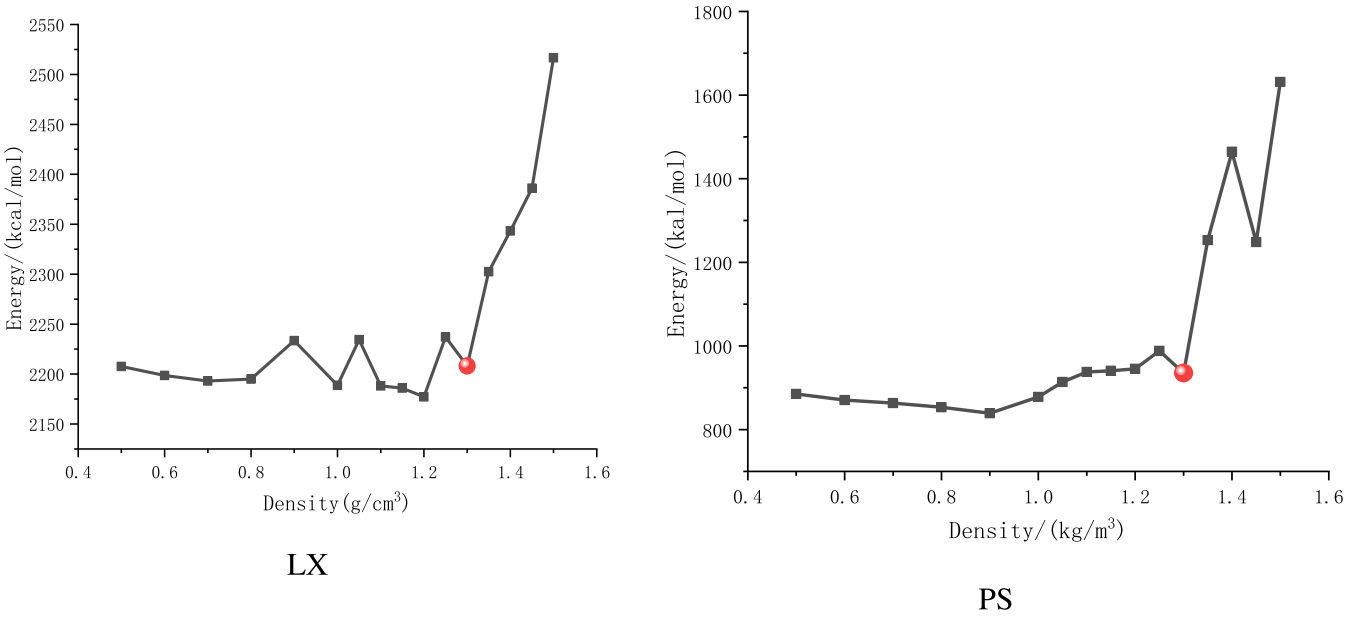

Figure 5. Relationship between total potential energy and calculated density.

parameters compared with the gas adsorption instrument, the instrument has a wider testing temperature area and can analyze more types of items.

According to the survey data,[29,30] the average geothermal gradient in the Liulin mining area is 278.05 K/100 m, and the average reservoir pressure gradient is 0.76 MPa/100 m. The average geothermal gradient in the Pingdingshan mining area is 281.95 K/100 m, and the average reservoir pressure gradient is 0.86 MPa/100 m. Combined with the purpose of the research and the actual situation of the experimental device, the maximum test pressure of the experiment in this paper is 11 MPa, and the test temperatures are 303.15, 323.15, 343.15, and 363.15 K. In the experiment, coking coal with a particle size of 3−6 mm was selected, the coal sample was dried and put into a sample tube, and the sample tube was installed in the sample test area of the instrument. The maximum adsorption equilibrium pressure was set to 11 MPa, and the experimental temperature was 303.15 K. The instrument automatically records the adsorption amount when adsorption equilibrium is reached, thereby obtaining the adsorption data at the adsorption equilibrium pressure point, and the experiment ends. The above experimental steps were repeated to carry out coking coal adsorption experiments at temperatures of 303.15, 323.15, 343.15, and 363.15 K, respectively. In this paper, experimental research on the isothermal adsorption characteristics of Liulin Xingwu coking coal and Pingdingshan No. 12 coking coal samples at a constant pressure of 11 MPa and different temperatures (303.15, 323.15, 343.15, and 363.15 K) was carried out, and a total of eight sets of experiments were carried out.

3. MOLECULAR SIMULATION TEST RESULTS AND ANALYSIS

3.1. Establishment of the Coal Structure Model. The author established a macromolecular model of coking coal in the Liulin Xingwu Coal Mine and Pingdingshan No. 12 Coal Mine according to the literature,[31,32] and the results are shown in Figure 3. The model structures of the two are mainly composed of aliphatic side chains, aliphatic bridge bonds, and aromatic skeleton structures. The correct combination of the types of aromatic carbon atoms and the distribution of the aliphatic carbon structure can reasonably characterize the molecular structure of coking coal. Therefore, this paper directly cited the molecular structure of coking coal for further study.

3.2. Coal Molecular Optimization and Boundary Determination. Geometric optimization and annealing optimization are performed on the initial model using the Geometric Optimization and Anneal items in Materials Studio. The precision is set to Fine, the force field is selected to

https://doi.org/10.1021/acsomega.2c06593
ACS Omega 2023, 8, 3129−3147

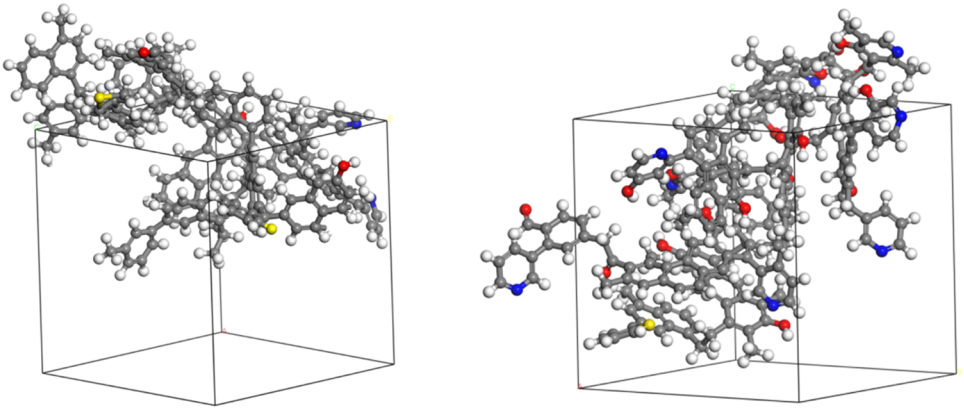

Figure 6. Coking coal structure model after incorporating periodic boundary conditions.

COMPASS, and the charge is selected to USE Current. The geometric optimization is usually conducted 5−10 times, and the number of annealing cycles is set as 10. After each cycle, a molecular configuration is output, and the molecular structure is optimized to obtain the geometrically most stable energy configuration and the annealed most stable energy configuration.[33]

The lowest energy structure of the coking coal molecule after geometry optimization (Figure 4a) and annealing (Figure 4b) is shown in Figure 4. The optimized structural model reaches the lowest energy and the most stable state, with twist and deformation, good three-dimensional structure, and all aromatic layered structures existing in the form of parallel and overlapping. To clarify the change characteristics of the coking coal molecular structure model before and after simulated annealing, the potential energy parameters of the coking coal molecular structure model before and after annealing were compared. The results are shown in Tables 3 and 4.

Both the bonding and nonbonding energies of the annealed coking coal molecular structure were significantly reduced. In terms of nonbonding energy, the van der Waals energy is smaller than the electrostatic energy, which indicates that the reduction in van der Waals energy determines the reduction in nonbonding energy. The reduction in bond energy depends on a large reduction in bond energy, bond angle energy, bond torsion energy, and bond inversion energy because the molecular structure model of coking coal has obvious torsion and deformation after annealing optimization.

3.2.1. Best Density Choice. Density is one of the most basic physical properties of coal and rock, and it is an important basis for evaluating whether the coal rock structure model is reasonable.[34] The periodic boundary conditions of coking coal macromolecules are established by the Amorphous Cell calculation module in Materials Studio.[35,36] The simulated density was set in the range of 0.5−1.5 g/cm^3. To choose the optimal density, the density increase step in the range of 0.5−1 g/cm^3 was set to 0.1 and the density increase step in the range of 1−1.5 g/cm^3 was set to 0.05.

On the basis of the above density settings, the cell size is continuously adjusted to obtain the variation law of the potential energy of the structural model under different periodic conditions, that is, the relationship between density and potential energy.

As shown in Figure 5, relevant literature[37,38] shows that the density of the lowest energy configuration cannot represent the true density of coal, and the lowest point of local energy after the lowest energy configuration should be the density of coal under formation conditions. The simulation results show that when the molecular density of LX coking coal is 1.0 g/cm^3, the energy reaches the lowest point; when the density is 1.3 g/cm^3, the energy increases sharply. Therefore, the final density of the LX coking coal molecular model is 1.3 g/cm^3. When the molecular density of PS coal is 0.9 g/cm^3, the energy reaches the lowest point; when the density is 1.3 g/cm^3, the energy increases sharply. Therefore, the final density of the PS coking coal molecular model is 1.3 g/cm^3. According to related literature,[39,40] the measured density range of coking coal is 1.15−1.50 g/cm^3. Therefore, the coal molecular densities simulated by LX and PS coking coals are reasonable. The crystal structure model is shown in Figure 6.

3.3. Construction of the Adsorbate. The best energy configuration of the adsorbent under the periodic boundary condition of the coking coal molecular structure is adopted. The adsorbate is CH_4. First, CH_4 is drawn under the MS software Visualizer module. After geometric optimization, energy optimization, and annealing, CH_4 with neutral surface charge and minimum energy is obtained. The parameter settings are consistent with the molecular structure of coking coal in the previous chapter. The CH_4 molecular structure model is shown in Figure 7.

4. RESULTS AND DISCUSSION

4.1. Experimental Results and Analysis. *4.1.1. Laboratory Measurement Isotherm Adsorption Line.* The adsorption amount directly obtained by the isotherm adsorption experiment is the excess adsorption amount (as

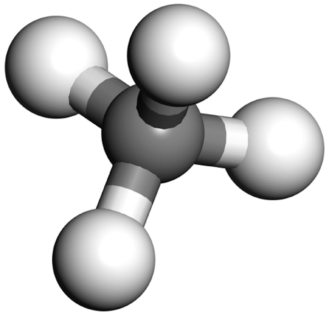

Figure 7. Methane molecular model.

https://doi.org/10.1021/acsomega.2c06593
ACS Omega 2023, 8, 3129−3147

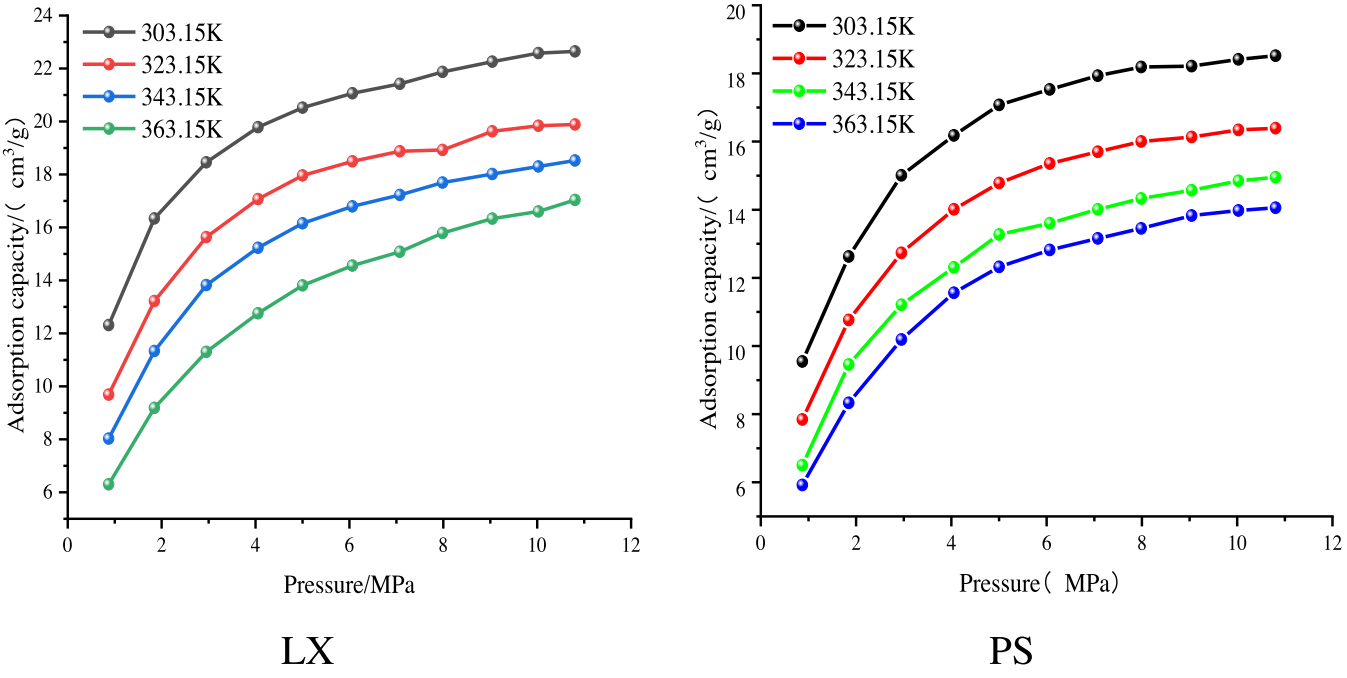

Figure 8. Isotherm adsorption line.

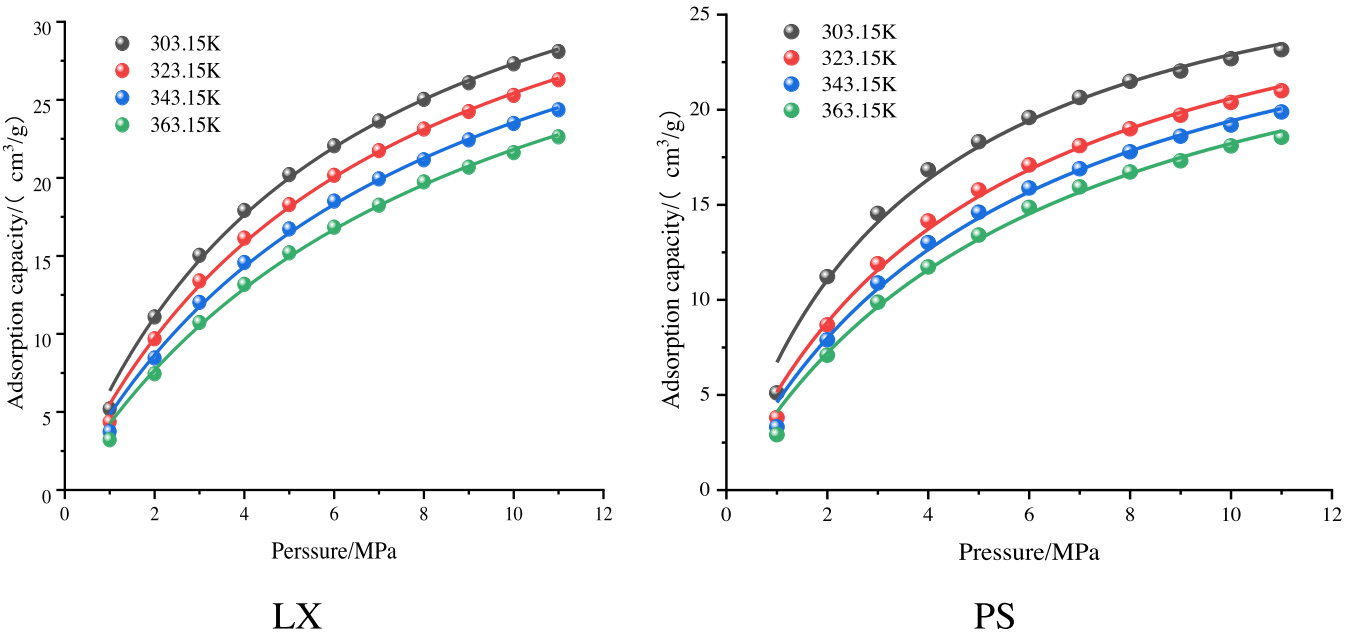

Figure 9. Simulate absolute adsorption capacity.

shown in Figure 8). The excess adsorption amount represents the adsorption amount left by the actual adsorption-phase density minus the gas-phase density. It can be seen from Figure 8 that under the conditions of constant temperature and 0−11 MPa pressure, the methane adsorption of coal samples increases with increasing pressure, which can be roughly divided into two stages: rapid increase and slow increase. The reasons for this phenomenon are as follows: The adsorption equilibrium of gas is a dynamic equilibrium process of adsorption and desorption. Thus, under the influence of the adsorption force, the free gas is adsorbed, and under the influence of the molecular force, the adsorbed gas overcomes the physical adsorption force and desorbs into the free gas. With increasing adsorption pressure, the probability of gas molecules impinging on the pore surface of the coal body increases, and the adsorption speed is accelerated, resulting in an increase in gas adsorption. As the gas adsorption pressure continues to increase, the distance between molecules decreases, the gas and coal surface molecules repel each other, and the force between them is repulsive. The larger the repulsive force, the less easily the gas is adsorbed on the coal surface, which shows that the gas adsorption rate decreases in this pressure range.

At constant pressure with increasing temperature, the adsorption capacity of coking coal gas decreases. This is because the adsorption of gas by coal samples is an exothermic

https://doi.org/10.1021/acsomega.2c06593
ACS Omega 2023, 8, 3129−3147

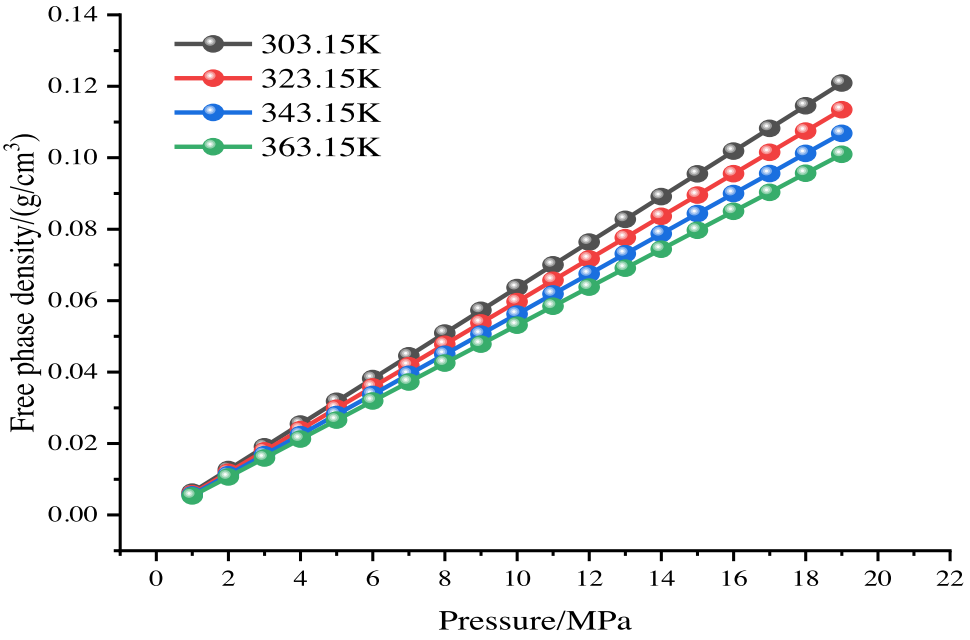

Figure 10. Relationship between methane free phase density and pressure.

Table 5. Commonly Used Adsorption-Phase Density Calculation Methods[a]

calculation method		formula to calculate
constant approximation method	Van der Waals constant approximation	$\rho_a = \frac{MRT_C}{8p_c}$
	approximate density of liquid at atmospheric boiling point	$\rho_a = \rho_{lp}$
	critical density approximation	$\rho_a = \rho_c$
Ozawa empirical formula method		$\rho_a = \rho_b \exp[-0.0025 \times (T - T_b)]$
excess adsorption capacity curve equation fitting method	Langmuir equation fitting	$n_{ex} = \frac{n_{abL}p}{p_{abL} + p}\left(1 - \frac{\rho_g}{\rho_a}\right)$
	L−F equation fitting method	$n_{ex} = \frac{n_{ab}(bp)^m}{1 + (bp)^m}\left(1 - \frac{\rho_g}{\rho_a}\right)$
	linear fitting of the descending section of the curve	$n_{ex} = a + b\rho_g$

[a]Note: ρ_a is the adsorption-phase density, g/cm^3; M is the molecular mass of the gas, g/mol; R is the universal gas constant, J/(mol*k); Tc is the critical temperature, K; P_c is the critical pressure, Pa; ρ_{lp} is the density of the liquid phase at the normal pressure boiling point, g/cm^3; ρ_c is the critical density, g/cm^3; ρ_b is the boiling point density, g/cm^3; T_b is the boiling temperature, K; n_{ex} is the excess adsorption capacity, cm^3/g; n_{abL} is the Rankine volume of absolute adsorption capacity, cm^3/g; and p_{abL} is the Rankine pressure of the excess adsorption capacity, MPa.

reaction. With increasing temperature, the activation energy of methane molecules increases, and the number of methane molecules adsorbed on the coal surface per unit time is smaller than the number of methane molecules detached from the coal surface during the same time. The final effect is the reduction of the ultimate adsorption capacity.

4.2. Molecular Simulation Isothermal Adsorption Line. Because the adsorption amount obtained by simulation is absolute adsorption (Figure 9), the adsorption amount measured by the laboratory is the excess adsorption amount. To verify the feasibility of the model, the absolute adsorption amount obtained by simulation should be transformed into excess adsorption amount, and the simulation results and experimental results should then be compared and analyzed.

4.2.1. Conversion of Absolute Adsorption Capacity. According to the definition of absolute adsorption capacity, the following relationship exists between excess adsorption capacity and absolute adsorption capacity[41]

$$V_{ad} = \frac{V_{ex}}{1 - \frac{\rho_g}{\rho_a}} \quad (1)$$

where V_{ad} is the excess adsorption capacity, cm^3/g; V_{ex} is the absolute adsorption capacity, cm^3/g; ρ_g is the density of gas phase, g/cm^3; and ρ_a is the density of adsorbed phase, g/cm^3.

According to eq 1, the density of the free phase (ρ_g) and the density of the adsorbed phase (ρ_a) must be determined to achieve the conversion from excess adsorption to absolute adsorption.

The free phase density can be calculated by the formula $PV = nRT$. The free phase density of methane in the temperature range of 303.15−363.15 K and equilibrium pressure range of 0−20 MPa is shown in Figure 10. As seen from Figure 10, since the simulated temperature has exceeded the critical temperature of methane, when the equilibrium pressure is greater than the critical pressure, methane transforms from the gaseous to the supercritical state, and the methane density does not change sharply during the phase-state transition. At the

https://doi.org/10.1021/acsomega.2c06593
ACS Omega 2023, 8, 3129−3147

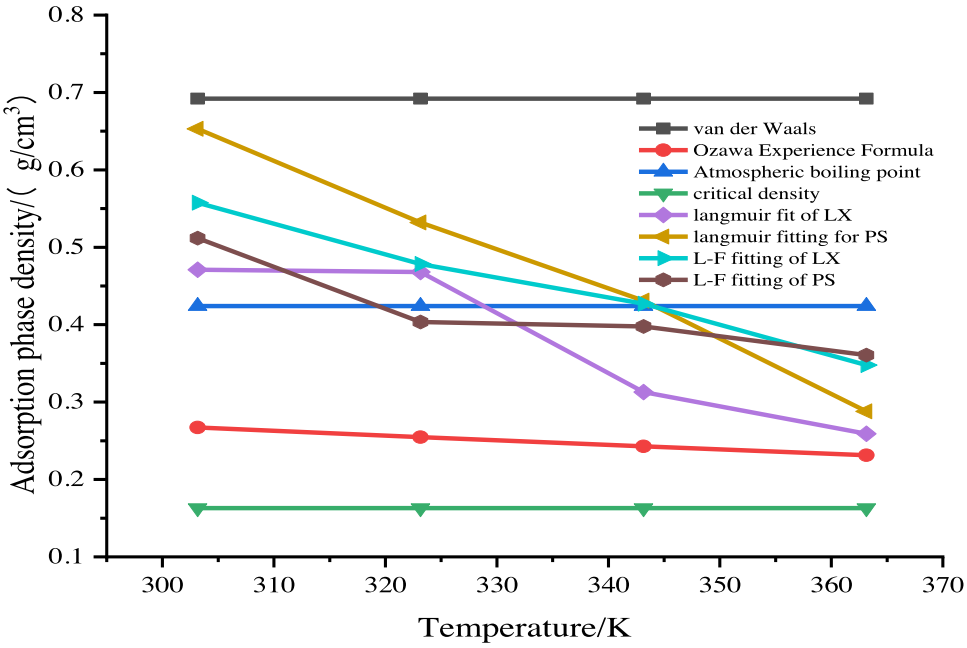

Figure 11. Relationship between methane adsorption-phase density and temperature.

same time, with increasing pressure, the difference in methane density at different temperatures becomes more obvious.

Under supercritical conditions, the adsorption-phase density cannot be measured directly, so it is mainly calculated by theoretical estimation and equation fitting. The commonly used calculation methods of adsorption-phase density (Table 5) mainly include the approximation method, empirical formula method, and excess adsorption amount curve fitting method.[42,43] The selection of the calculation method of the adsorption-phase density has a great influence on the correction result of the absolute adsorption amount. Therefore, considering the accuracy of the correction result of the absolute adsorption amount, it is necessary to correct the calculation method of the adsorption-phase density.

In the range of supercritical temperature, adsorbent molecules lose their average translational energy due to the effect of adsorption potential but still have high rotational and vibrational energy. Therefore, the density of the adsorbent phase under supercritical conditions should be between the critical density and the density of the liquid at the atmospheric boiling point.[44] In addition, the absolute adsorption capacity is theoretically monotonic and does not have a maximum value. Therefore, the rationality of the different adsorption-phase density estimation methods in Table 5 can be verified from two perspectives: the value range of the adsorption-phase density and the monotonicity of the absolute adsorption amount. Figure 11 shows the relationship curve of the methane adsorption-phase density and temperature calculated using different adsorption-phase density methods. Figure 11 shows that within the temperature range of 303.15−363.15 K, the approximate value of the atmospheric boiling point density of methane is 0.424 g/cm^3, and the approximate value of the critical density is 0.163 g/cm^3. Therefore, the adsorption-phase density of methane should be between 0.163 and 0.424 g/cm^3. The methane adsorption-phase density calculated by the van der Waals formula is 0.692 g/cm^3, which is not within a reasonable range. The methane adsorption-phase density obtained by Ozawa's empirical formula method is 0.267−0.231 g/cm^3, which is within a reasonable range, and the adsorption-phase density decreases with increasing temperature. Since the temperature is 303.15−363.15 K and pressure is 0−11 MPa, the experimental data do not show a point of decline, so the linear fitting of the descending section of the curve cannot be used to obtain the adsorption-phase density in this paper. The adsorption-phase density obtained by the L−F regression method is between 0.3 and 0.6 g/cm^3, and the calculation result is within a reasonable range only in the temperature range of 323.15−363.15 K; the adsorbed phase densities obtained by the Langmuir equation regression method are only within a reasonable range in the temperature range of 343.15−363.15 K.

Therefore, the Ozawa empirical formula was used to calculate the adsorption-phase density of methane in this paper. The comparison between the simulation results and the experimental results is shown in Figure 12.

Figure 12 shows that the adsorption capacity of LX coking coal and PS coking coal molecules in the range of 0−11 MPa obtained by molecular simulation tends to be consistent with the change in laboratory test results, the consistency between them is high, and the difference between them decreases with increasing temperature and pressure. It can be considered that the simulation results of the molecular chemical structure model of coking coal are reliable under the set parameters.

4.3. Isothermal Adsorption Simulation under High Temperature and High Pressure. According to Section 3.2, the simulation results of the established molecular structure model of coking coal are reliable under the set parameters. To compensate for the limitations of the experimental temperature and pressure of the Hsorb-2600 high-temperature and high-pressure gas adsorption instrument, a molecular dynamics simulation method was used to study the influence of high temperature and high pressure on coking coal adsorption under the conditions of a maximum adsorption equilibrium pressure of 20 MPa and temperatures of 303.15, 323.15, 343.15, and 363.15 K. The simulation results are shown in Figure 13.

https://doi.org/10.1021/acsomega.2c06593
ACS Omega 2023, 8, 3129−3147

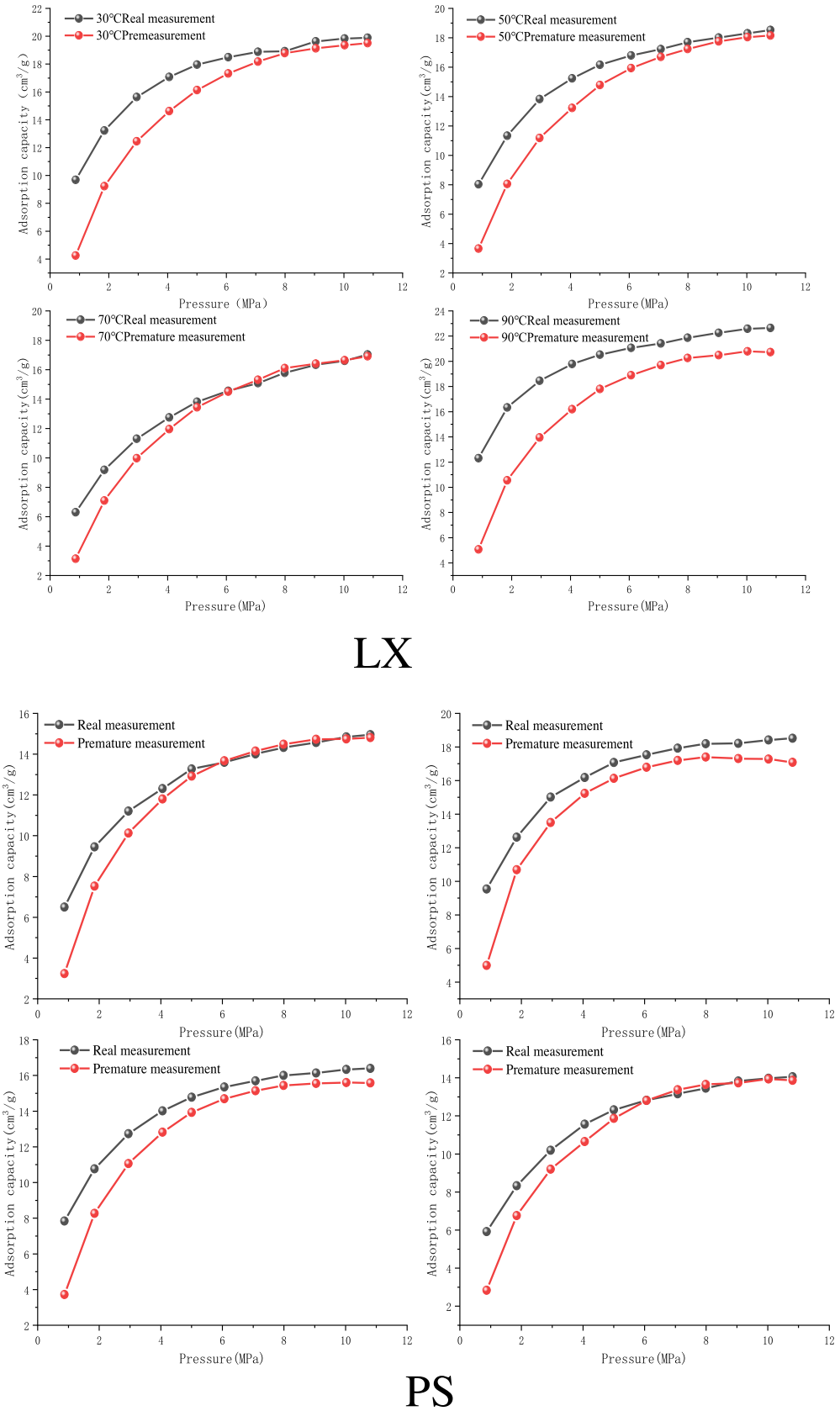

Figure 12. Comparison between molecular simulation and experimental results.

As shown in Figure 13, with increasing pressure, the adsorption capacity of gas increases rapidly in the early stage of adsorption. In the middle stage of adsorption, the gas adsorption capacity appeared to be transiently stable. At the later stage of adsorption, the amount of gas adsorption decreases. This is because in the early stage of adsorption, with

https://doi.org/10.1021/acsomega.2c06593
ACS Omega 2023, 8, 3129−3147

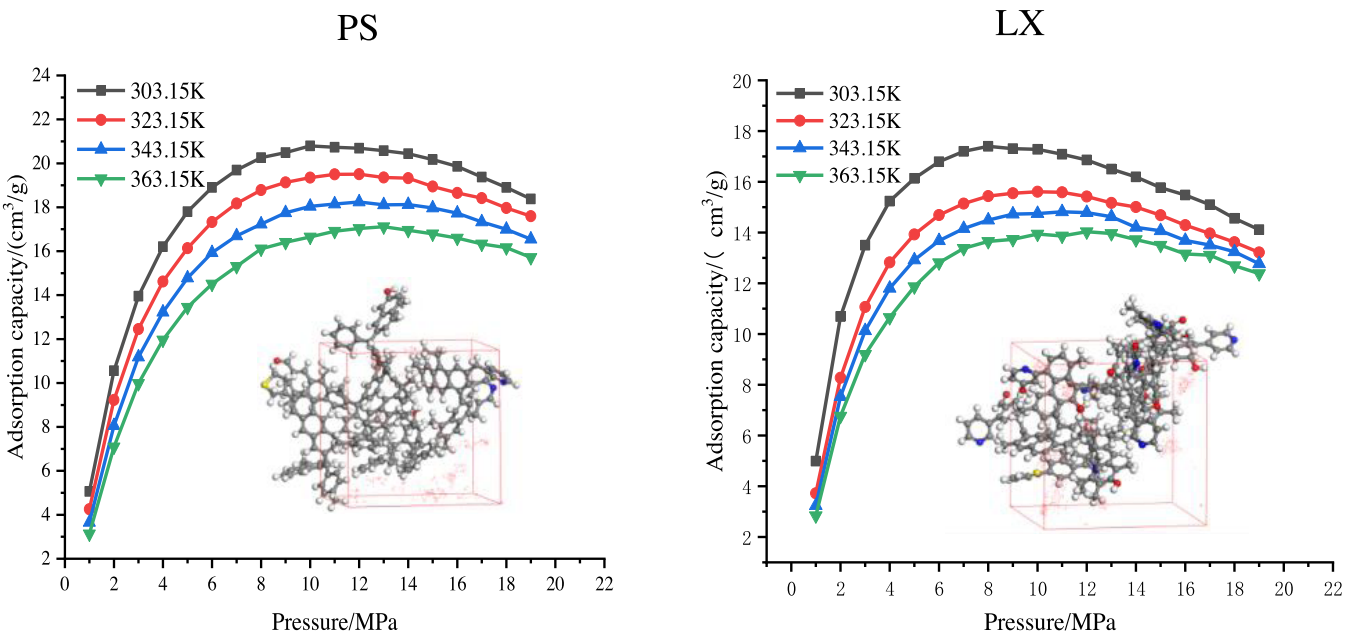

Figure 13. Simulated adsorption isotherm.

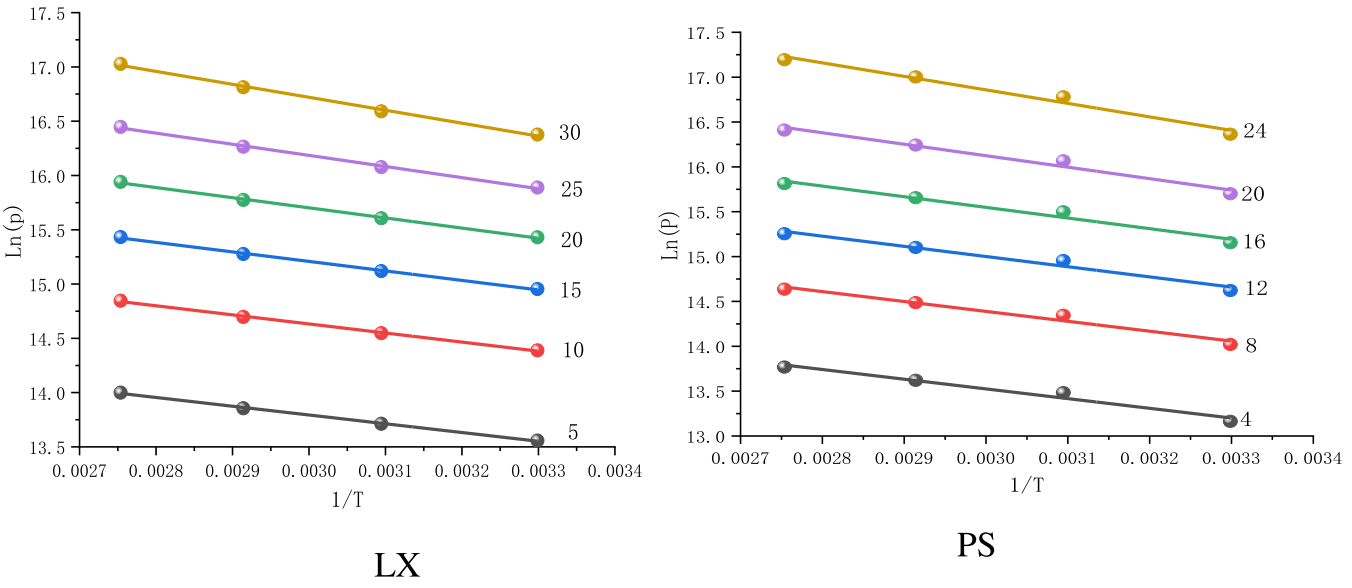

Figure 14. Relationship between Ln P and $1/T$ corresponding to different adsorption capacities of each coal sample.

the increase in adsorption pressure, the density of the free phase increases, the density of the adsorbed phase increases continuously, and the excess adsorption capacity increases accordingly. When the adsorption pressure increases to just the adsorption saturation, the adsorption density increases to the maximum value, and the excess adsorption amount reaches the maximum value at this time, that is, the peak of the isotherm. In the late stage of adsorption, after adsorption saturation occurs, the pressure continues to increase, and the density of the free phase continues to increase, but the density of the adsorbed phase tends to be stable and does not change, and the excess adsorption must decrease linearly.

When the pressure is the same, the excess gas adsorption of coal samples decreases with increasing temperature, but the decrease range is not obvious in the high-pressure section. This is because the adsorption vacancies in the coking coal molecules are almost saturated under the high-pressure section, and the temperature increases at this time. The kinetic energy of methane molecules can be increased, and the adsorbed methane molecules can escape from the weaker adsorption sites of the coal molecules. However, due to the existence of a large number of adsorption vacancies in the low-pressure section, the adsorbed methane molecules are strongly attracted by the wall surface, and it becomes more difficult for them to escape.

4.4. Isosteric Heat of Adsorption. Adsorption heat is the comprehensive result of energy changes in the adsorption process, which reflects the strength of the adsorption of the adsorbate by the adsorbent. It can be used to judge the type of adsorption and analyze the heterogeneity of the adsorbent surface.

At present, the calculation of adsorption heat mainly includes direct calorimetry, the Clausius−Clapeyron equation method, gas chromatography, etc.[45]

https://doi.org/10.1021/acsomega.2c06593
ACS Omega 2023, 8, 3129−3147

Table 6. Equation of Isometric Adsorption Line and Isometric Adsorption Heat of Each Coal Sample

coal sample	adsorption capacity (cm^3/g)	linear equation	correlation coefficient	isosteric heat of adsorption (KJ/mol)
LL	5	$Y = -807.25*X + 16.2155$	0.99773	6.7113
	10	$Y = -836.11*X + 17.14084$	0.99766	6.9513
	15	$Y = -875.64*X + 17.83547$	0.99754	7.280
	20	$Y = -933.15*X + 18.50157$	0.99729	7.758
	25	$Y = -1024.57*X + 19.25881$	0.99676	8.518
	30	$Y = -1192.71*X + 20.29848$	0.99538	9.916
PD	4	$Y = -1181.68*X + 16.77007$	0.95703	8.993
	8	$Y = -1103.64*X + 17.69994$	0.95783	9.175
	12	$Y = -1135.59*X + 18.40742$	0.95896	9.441
	16	$Y = -1186.32*X + 19.10738$	0.96069	9.863
	20	$Y = -1279.34*X + 19.96\ 235$	0.96386	10.636
	24	$Y = -1505.92*X + 21.37548$	0.97027	12.520

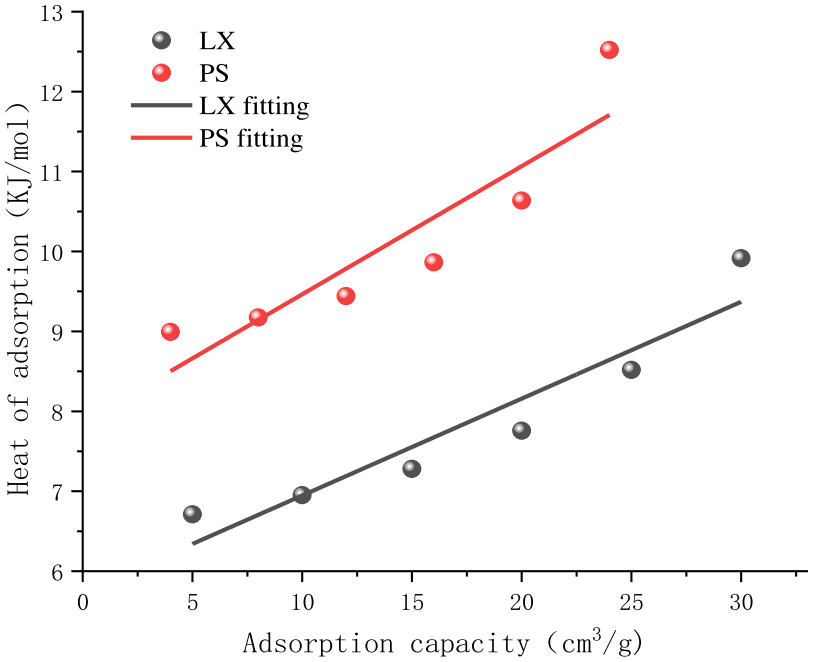

Figure 15. Relationship between adsorption capacity and adsorption heat.

The direct method uses a calorimeter attached to the adsorption equipment to measure the adsorption heat. Although the adsorption heat can be measured directly, it is only suitable for measuring the adsorption process with greater specific heat. Gas chromatography is used to calculate the heat of adsorption by measuring the time and retention volume of gas in coal. This method will cause large errors in the determination of the volume of gas adsorbed on coal. Generally, the Clausius−Clapeyron equation method is used to calculate the adsorption heat. The adsorption heat is obtained by measuring the corresponding pressure and temperature under the same adsorption amount and plotting with Ln P and $1/T$ as coordinates. The equation is as follows[46]

$$\left(\frac{\partial \mathrm{Ln}\, P}{\partial T}\right)_{\tau} = \frac{Q_{st}}{RT^2} \tag{2}$$

Equation 2: T integral of left and right sides.

$$\mathrm{Ln}P = -\frac{Q_{st}}{RT} + C \tag{3}$$

where Q_{st} is the equal adsorption heat, KJ/mol; T is the temperature, K; P is the pressure, MPa; R is the gas constant, 8.314; and C is a constant.

Taking a different adsorption amount between each group of coal samples (since the selected adsorption amount should cover the whole adsorption process, the selected adsorption amount of different coal samples should also be different), the adsorption capacity of coking coal in the LX mine is on the high side, so the value is on the high side. The adsorption capacity of PS mine coking coal is generally low, so the value is low. Since the two groups of coal samples cannot obtain the same adsorption capacity value in their respective simulation results at different temperatures, it is necessary to bring the set adsorption capacity of each group into the fitting curve in Figure 9 to obtain the corresponding pressure. The logarithm of the obtained pressure is calculated, Ln P and $1/T$ are used as the ordinates and abscissa for drawing, respectively, and Origin software is used to fit them. The fitting results are shown in Figure 14. It can be seen from eq 3 that the slope of the line is the ratio of the equivalent adsorption heat and the gas constant, and the slope multiplied by the gas constant is the equivalent adsorption heat. The fitting equation, correlation

https://doi.org/10.1021/acsomega.2c06593
ACS Omega 2023, 8, 3129−3147

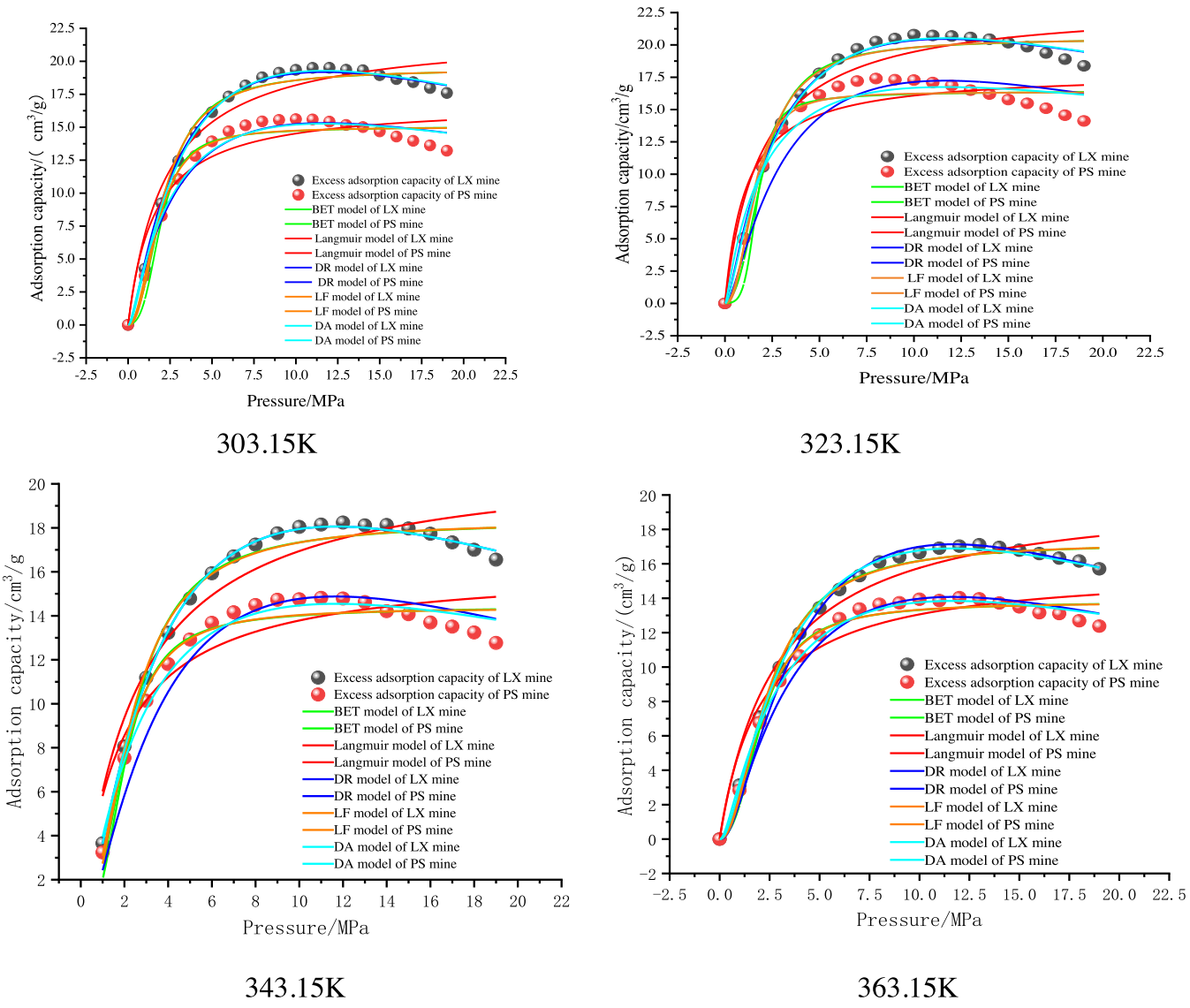

Figure 16. Fitting effects of different adsorption models.

Table 7. Langmuir and L−F Adsorption Models

		adsorption model						
		Langmuir[a]			L−F[b]			
coal sample	temperature (K)	n_0	b	R^2	n_0	b	n	R^2
LX	303.15	23.196	0.5217	0.9354	20.4897	0.2693	2	0.9780
	323.15	22.2521	0.4475	0.9435	19.4009	0.2302	2	0.9825
	343.15	21.2276	0.3953	0.9081	18.2945	0.2029	2	0.9735
	363.15	20.2645	0.3501	0.9557	17.2666	0.1818	2	0.9887
PS	303.15	17.901	0.8826	0.8654	16.3458	0.3731	2	0.9446
	323.15	16.8391	0.6287	0.8969	14.9884	0.2596	2	0.9634
	343.15	16.2755	0.5536	0.8237	14.3411	0.2347	2	0.9435
	363.15	15.7768	0.4807	0.9262	13.7458	0.2127	2	0.9783

[a] $n_{ab} = \frac{n_0 \times b \times p}{1 + b \times p}$. [b] $n_{ab} = \frac{n_0 \times (b \times p)^n}{1 + (b \times p)^n}$.

coefficient, and calculated equivalent adsorption heat are shown in Table 6, which shows that the adsorption heat range of the Liulin Xingwu coking-free coal sample is 6.7−10 kJ/mol. The adsorption heat range of coking coal samples of the No. 12 Coal Mine in Pingdingshan is 8.9−12.6 kJ/mol, and the adsorption heat in the whole adsorption process is less than the upper limit of the general physical adsorption heat of 40 kJ/mol,[47] while the adsorption heat range in the chemical adsorption process is 84−600 kJ/mol. Thus, the adsorption of methane by coking coal belongs to physical adsorption, and it is a spontaneous exothermic process.

https://doi.org/10.1021/acsomega.2c06593
ACS Omega 2023, 8, 3129−3147

Table 8. D−A and D−R Adsorption Models

		adsorption model						
		D−A[a]				D−R[b]		
coal sample	temperature (K)	n_0	D	n	R^2	n_0	D	R^2
LX	303.15	20.4571	0.2104	2	0.9938	20.5229	0.2182	0.9944
	323.15	19.1849	0.2293	2	0.9974	19.2881	0.2433	0.9981
	343.15	18.0595	0.2652	2	0.9979	18.0595	0.2652	0.9980
	363.15	17.1362	0.3472	2	0.9895	16.8925	0.2879	0.9982
PS	303.15	17.2335	0.25	2	0.8721	16.7413	0.1548	0.9397
	323.15	15.3214	0.21	2	0.9748	15.2467	0.1985	0.9762
	343.15	14.877	0.3	2	0.9084	14.5448	0.2158	0.9701
	363.15	14.0759	0.3	2	0.9781	13.8412	0.2368	0.9933

[a] $n_{ab} = n_0 \exp\left\{-D\left[\ln\left(\frac{p_0}{p}\right)\right]^n\right\}$. [b] $n_{ab} = n_0 \exp\left\{-D\left[\ln\left(\frac{p_0}{p}\right)\right]^2\right\}$.

Figure 15 shows that the adsorption heat of the two groups of coking coal for methane gas increases with increasing adsorption capacity, and the relationship between the two is linear. This is due to the influence of the heterogeneity of the adsorbent surface and the force between adsorbent molecules. The heterogeneity of the adsorbent surface determines that the adsorbent molecules first preferentially adsorb at the highly active sites and then gradually adsorb at the weakly active sites, and an increasing number of methane molecules are adsorbed. The mutual repulsion between methane molecules becomes increasingly stronger, and an increasing amount of energy is released, which causes the adsorption heat to increase with increasing adsorption amount.

5. ISOTHERMAL ADSORPTION MODEL OF COKING COAL UNDER HIGH-TEMPERATURE AND HIGH-PRESSURE CONDITIONS

5.1. Classical Adsorption Model and Adsorption Theory. To accurately describe the methane adsorption characteristics under high-temperature and high-pressure conditions, this paper selected for research the most representative of the adsorption models among the Langmuir monolayer model, BET multimolecular layer model, L−F adsorption model, and micropore filling mode[48−50] based on the adsorption potential theory.

Table 9. BET Adsorption Model

		BET[a]		
coal sample	temperature (K)	n_0	c	R^2
LX	303.15	6.8905	3	0.9317
	323.15	7.1248	2	0.8987
	343.15	7.0758	2	0.9216
	363.15	7.0719	2	0.9654
PS	303.15	2.9809	5	0.8690
	323.15	3.9313	4	0.8263
	343.15	4.2402	3	0.8668
	363.15	4.5702	3	0.9469

[a] $n_{ab} = \frac{n_0 \times c \times p}{(p_0 - p)[1 + (c-1)p/p_0]}$.

Table 10. Adsorption Capacity at Different Depths

coal sample	temperature (K)	buried depth (m)	adsorption capacity (cm^3/g)
LX	303.15	800	19.31
	323.15	1200	18.99
	343.15	1800	18.05
	363.15	2300	16.76
PS	303.15	400	13.28
	323.15	700	13.46
	343.15	1000	13.61
	363.15	1200	13.08

(1) Langmuir monolayer model

$$n_{ab} = \frac{n_0 \times b \times p}{1 + b \times p} \tag{4}$$

(2) L−F model

$$n_{ab} = \frac{n_0 \times (b \times p)^n}{1 + (b \times p)^n} \tag{5}$$

(3) BET multimolecular layer model

$$n_{ab} = \frac{n_0 \times c \times p}{(p_0 - p)[1 + (c-1)p/p_0]} \tag{6}$$

(4) D−R model

$$n_{ab} = n_0 \exp\left\{-D\left[\ln\left(\frac{p_0}{p}\right)\right]^2\right\} \tag{7}$$

(5) D−A model

$$n_{ab} = n_0 \exp\left\{-D\left[\ln\left(\frac{p_0}{p}\right)\right]^n\right\} \tag{8}$$

where n_{ab} is the excess adsorption capacity, cm^3/g; n_0 is the limit adsorption capacity, cm^3/g; b is a constant related to the adsorbent, adsorbate properties, and temperature, MPa^{-1}; c, n, and D are coefficients; p is the pressure, MPa; and p_0 is the saturated vapor pressure, MPa.

5.2. Comparison of Fitting Effects of Adsorption Models. In this paper, five representative adsorption models are fitted to the excess adsorption capacity, and the fitting results are shown in Figure 16. The fitting parameters of each model are shown in Tables 7−9. It can be seen from the table that the saturated adsorption amount n_0 and the micropore filling n_0 have the same change trend as the adsorption isotherm. The adsorption capacity of methane decreases with increasing temperature because the gas adsorption of coal

https://doi.org/10.1021/acsomega.2c06593
ACS Omega 2023, 8, 3129−3147

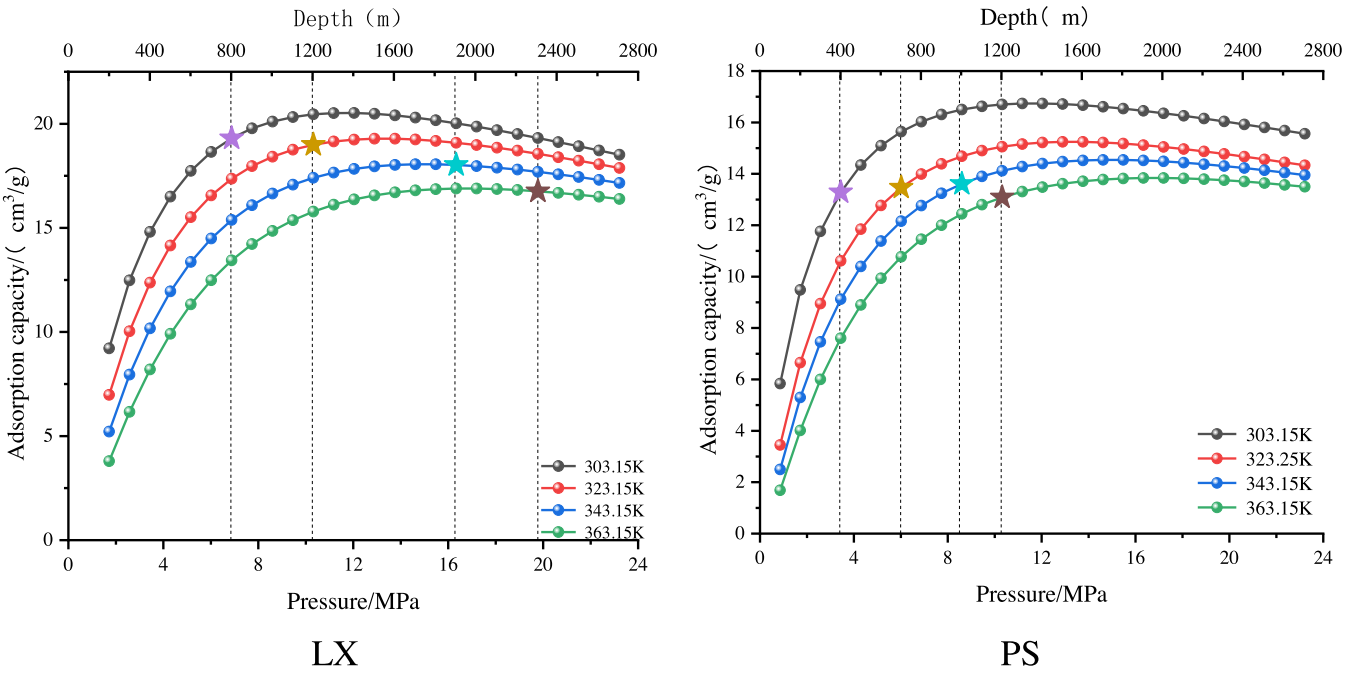

Figure 17. Prediction of adsorption capacity at different depths.

Table 11. Fitting Results of Isothermal Adsorption Data for Coking Coal Samples

coal sample	A	D	E_A	R^2
LX	3.899	0.004	56.932	0.998
PS	3.893	0.003	49.081	0.996

samples is an exothermic reaction. As the temperature increases, the activation energy of methane molecules increases, and the number of methane molecules adsorbed on the coal surface per unit time is less than the number of methane molecules detached from the coal surface during the same period. The effect is manifested as a decrease in the limit of the adsorption capacity. With increasing temperature, the Langmuir pressure gradually decreased, indicating that the adsorption capacity of the inner surface of coal for methane gradually decreased. According to the relative error R^2 of each model in Tables 7−9, the D−R model of the micropore filling model based on adsorption potential theory has the best fitting effect, the D−A model and L−F model have moderate fitting effects, and the Langmuir model of monolayer adsorption theory and BET model of bilayer adsorption theory have the poorest fitting effects. The order of fit from good to bad is D−R > D−A > L−F > BET > Langmuir. The widely used Langmuir model does not fit well under supercritical conditions. The coal surface is highly heterogeneous, but the Langmuir equation assumes that adsorption occurs on isotropic and uniform adsorption surfaces, which results in a poor fitting effect. The BET equation is suitable for low pressure. The pressure in this experiment is high, which does not conform to the pressure range of this model, resulting in poor fitting results. The deep coking coal has a large proportion of micropores, and the structural stress damages the coal surface structure, thereby enhancing the roughness of the micropore surface. The D−R and D−A models based on micropore filling theory can better reflect the adsorption characteristics of coking coal. However, the fitting parameters of the D−R model can better reflect the adsorption characteristics of coking coal. According to the analysis results of the physical meaning of fitting parameters and the evaluation of the model fitting effect, the D−R model is relatively suitable for describing the supercritical adsorption behavior of coking coal and the study of the characteristics of supercritical adsorption.

5.3. Prediction of Methane Adsorption in Deep Coal Seams. *5.3.1. Model Derivation of Methane Adsorption by Deep Coking Coal.* Based on the simulation results of the methane adsorption isotherm by coking coal, combined with the geothermal gradient, the methane adsorption capacity of coal at a certain depth can be predicted. According to the investigation, the geothermal gradient of the Liulin Xingwu Coal Mine is 278.05 K/100 m and that of the Pingdingshan No. 12 Coal Mine is 281.95 K/100 m.[51−53] Combined with the isothermal adsorption data, a temperature−pressure−depth−methane adsorption curve can be drawn. Table 10 shows the methane adsorption corresponding to different burial depths in the Xingwu Coal Mine and Pingdingshan Coal Mine.

As can be seen from 5.2, D−R model is relatively suitable for supercritical adsorption of coking coal. When $P_0 = P_C \times \left[\frac{T}{T_c}\right]^2$ is substituted into (7), the comprehensive adsorption model of temperature and pressure is as follows

$$V = n_0 \times e^{[-D\times(2\times \mathrm{Ln}T - \mathrm{Ln}P + 12.04)^2]} \quad (9)$$

As the depth increases, the gas pressure and temperature change. From 1.2, the average reservoir pressure gradient in the Xingwu mining area in Shanxi is 0.76 MPa/100 m; the average reservoir pressure gradient in the Pingdingshan mining area in Henan is 0.86 MPa/100 m. Then, there are

LX

$$p = (h/100) \times 0.76 \quad (10)$$

PS

https://doi.org/10.1021/acsomega.2c06593
ACS Omega 2023, 8, 3129−3147

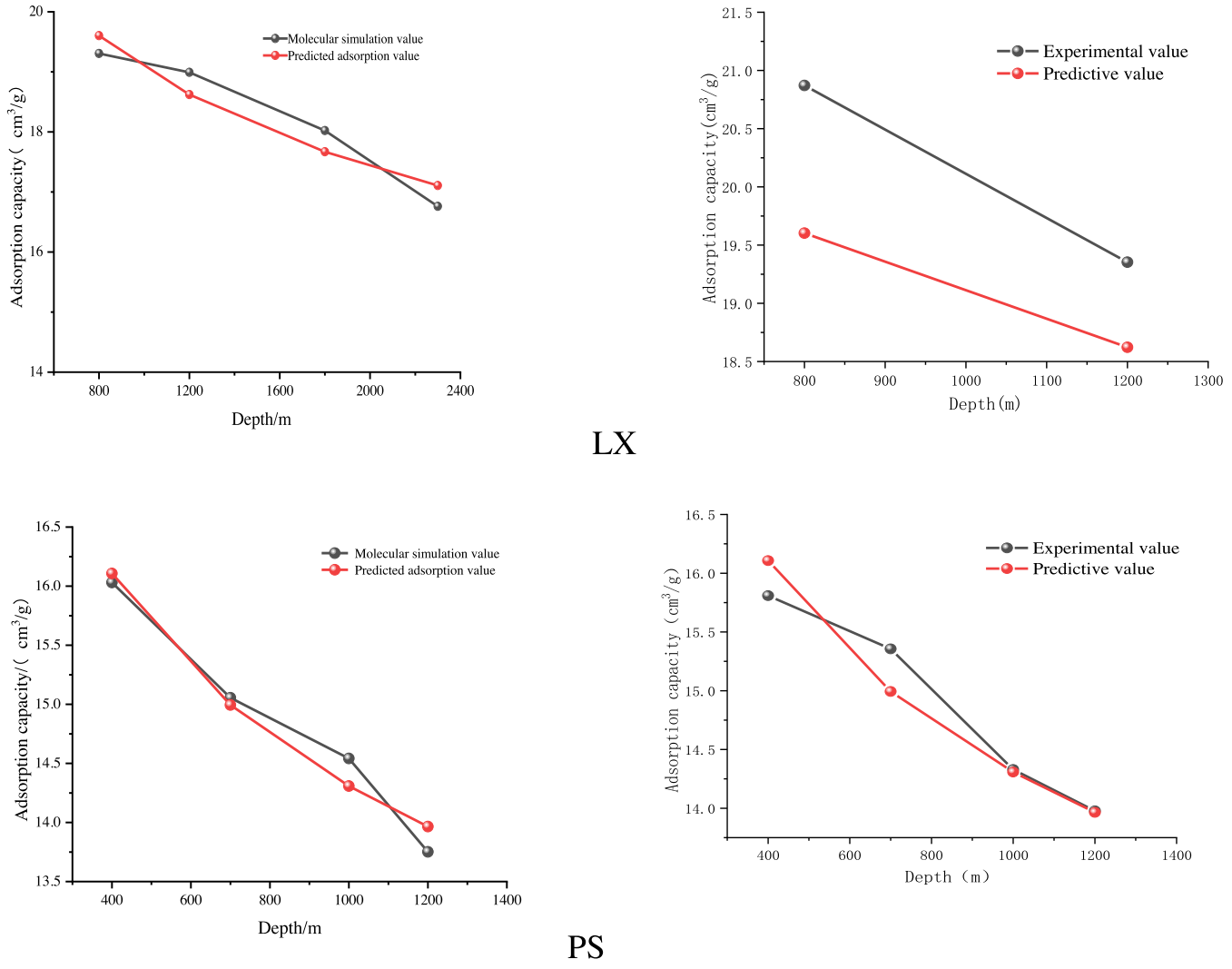

Figure 18. Comparison of predicted adsorption value and measured adsorption value.

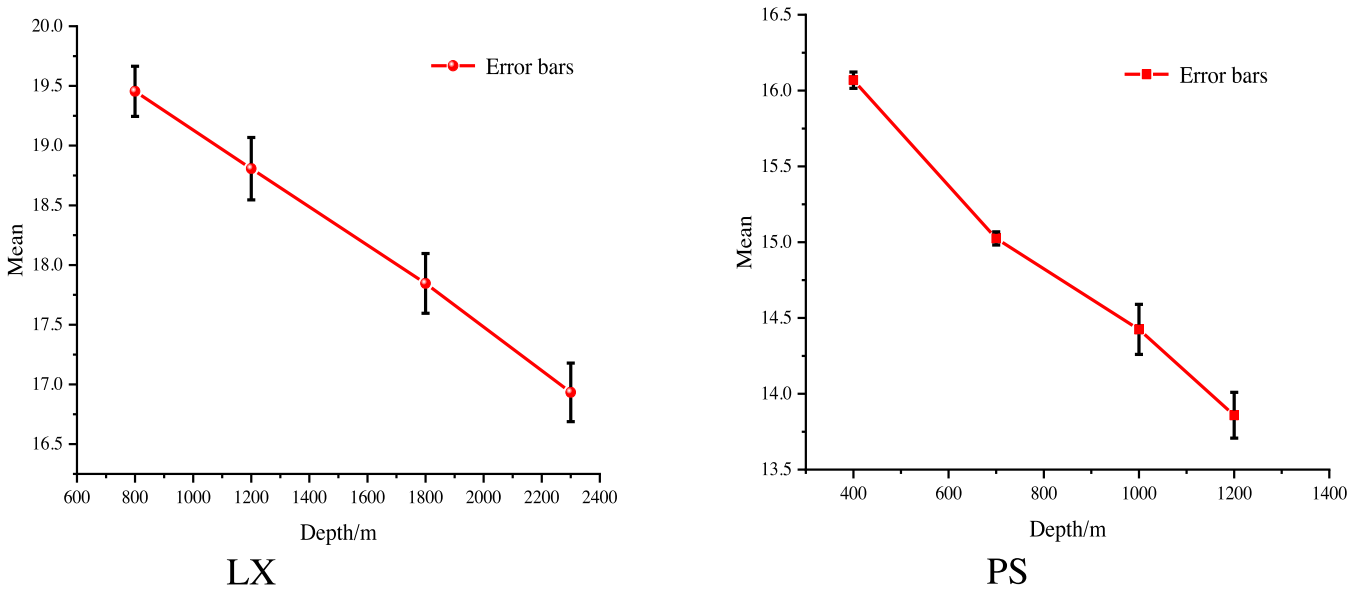

Figure 19. Error bars.

$$p = (h/100) \times 0.86 \quad (11)$$

where h is the burial depth (m).

https://doi.org/10.1021/acsomega.2c06593
ACS Omega 2023, 8, 3129−3147

Due to the positive relationship between the formation temperature and depth, the average geothermal gradient in Xingwu mining area in Shanxi is 278.05 K/100 m and that in Pingdingshan mining area in Henan is 281.95 K /100 m. Then, there are

LX

$$T = (h/100) \times 3.9 \tag{12}$$

PS

$$T = (h/100) \times 7.8 \tag{13}$$

where h is the burial depth (m).

On the basis of the adsorption model in which the adsorption gas volume of coking coal varies with temperature and pressure, eqs 10 and 12 and eqs 11 and 13 are substituted into the equation to obtain the calculation model of the adsorption gas volume of coking coal varying with depth. The model expression is

LX

$$V = n_0 \times e^{[-D\times(\mathrm{Ln}\,h+10.36)^2]} \tag{14}$$

PS

$$V = n_0 \times e^{[-D\times(\mathrm{Ln}\,h+11.7)^2]} \tag{15}$$

Taking the logarithm of both sides of the equation

LX

$$\mathrm{Ln}\,V = \mathrm{Ln}\,n_0 - D \times (\mathrm{Ln}\,h + 10.36)^2 \tag{16}$$

PS

$$\mathrm{Ln}\,V = \mathrm{Ln}\,n_0 - D \times (\mathrm{Ln}\,h + 11.7)^2 \tag{17}$$

In eqs 16 and 17, $\mathrm{Ln}\,n_0$ is considered as coefficient A. Isothermal adsorption data at different depths in Table 10 are used to calculate logarithm values of adsorption capacity, that is, Origin is used to plot and fit the relationship between Ln V and Ln h; then, the coefficients A and D can be known, n_0 can be obtained by exponentiating A, and then n_0 and D can be substituted into eqs 14 and 15. The calculation model of coal-adsorbed gas with depth can be obtained (Figure 17).

5.3.2. Validation of the Adsorption Model. The commonly used adsorption model has a good fitting effect on shallow coal seams, but poor fitting effect on deep coal seams. However, the current coking coal mining has tended to be deep, so it is particularly important to study the variation law of coal seam gas content with burial depth.

The calculation model of the variation of the amount of adsorbed gas in coking coal with depth derived based on this has a wide range of applications. To further verify the reliability of the model, eight groups of coking coal isotherm adsorption data were used to verify the model derived in this paper, and error bars were used to analyze the difference between the adsorption amount calculated by the model in this paper and the measured adsorption amount.

Eight groups of data in Table 10 are selected to verify the model: (1) Using the adsorption data of four groups of LX ore and PS ore at different depths, the logarithmic value of the adsorption amount, that is, ln V, is calculated and Origin is used to plot the relationship between ln V and Ln h, and then the coefficients A and D can be known (Table 11). (2) The exponent of the coefficient A is calculated to obtain n_0, and n_0 and D are put into eqs 14 and 15 to obtain the calculation model of the variation of the amount of gas adsorbed by coking coal in the two mines with depth. The results of the predicted adsorption amount and the measured adsorption amount are shown in Figure 18. Error bars are shown in Figure 19.

Figure 19 shows that the predicted values of coking coal samples from the LX mine and PS mine are in good agreement with the measured values, and the relative errors are both less than 10%. This shows that the calculation model of the adsorption gas volume of coking coal with the depth change proposed in this paper is of high accuracy and has certain feasibility. The final model is expressed as

$$\text{LX:}\quad V = 56.932 \times e^{[-0.0036\times(\mathrm{Ln}h+10.36)^2]} \tag{18}$$

$$\text{PS:}\quad V = 49.081 \times e^{[-0.0035\times(\mathrm{Ln}\,h+11.7)^2]} \tag{19}$$

6. CONCLUSIONS

(1) The adsorption data obtained by molecular dynamics simulation are in good agreement with the experimental data. The combination of simulation and experiment can better study the adsorption characteristics of coking coal to methane under supercritical conditions.

(2) Under supercritical conditions, the excess adsorption capacity of methane decreased with the increase of temperature. With the increase of pressure, the change of methane excess adsorption capacity is mainly divided into three stages: rapid increase in the early stage, transient stability in the middle stage, and decrease in the late stage.

(3) The heat of methane gas adsorption of Liulinxing Xinwu coking coal and Pingdingshan coal increases with the increase of adsorption capacity, and the relationship between them is linear.

(4) Based on the classical adsorption models, D−R has the best fitting effect, the D−A model and L−F model have moderate fitting effects, and the Langmuir model of monolayer adsorption theory and BET model of bilayer adsorption theory have the poorest fitting effect.

(5) Based on the D−R adsorption model, the adsorption characteristics of deep coking coal can be studied. Combined with the pressure gradient, temperature gradient, and adsorption isotherm, the amount of methane adsorption by coal at a certain depth can be predicted. After the Xingwu Coal Mine in Liulin, Shanxi, is 800 m deep, the adsorption capacity decreases with the increase of the depth. After the Pingdingshan Mine in Henan Province is 400 m deep, the adsorption capacity decreases with the increase of the depth.

AUTHOR INFORMATION

Corresponding Author

Shasha Si − *School of Safety Science and Engineering, Henan Polytechnic University, Jiaozuo, Henan 454000, China;* orcid.org/0000-0002-9909-3686; Email: 212001020012@home.hpu.edu.cn

Authors

Zhaofeng Wang − *School of Safety Science and Engineering, Henan Polytechnic University, Jiaozuo, Henan 454000, China; MOE Engineering Research Center of Mine Disaster Prevention and Emergency Rescue, Jiaozuo, Henan 454000, China; State Collaborative Innovation Center of Coal Work Safety and Clean-efficiency Utilization, Henan Polytechnic*

https://doi.org/10.1021/acsomega.2c06593
ACS Omega 2023, 8, 3129−3147

University, Jiaozuo, Henan 454000, China; orcid.org/0000-0003-2860-6963

Yongjie Cui − *National Energy Shendong Coal Group Buertai Coal Mine, Ordos, Inner Mongolia 017000, China*

Juhua Dai − *School of Safety Science and Engineering, Henan Polytechnic University, Jiaozuo, Henan 454000, China*

Jiwei Yue − *School of Safety Science and Engineering, Anhui University of Science and Technology, Huainan, Anhui 232001, China*

Complete contact information is available at: https://pubs.acs.org/10.1021/acsomega.2c06593

Author Contributions

Z.W. conceived the experiment, analyzed the results, and drafted the manuscript; S.S., Y.C., J.D., and J.Y. coordinated the study and helped draft the manuscript. All authors gave final approval for publication.

Notes

The authors declare no competing financial interest.

■ ACKNOWLEDGMENTS

This study was financially supported by the National Natural Science Foundation of China (52074107).

■ REFERENCES

(1) Wei, Q.; Li, X. Q.; Hu, B. L.; Zhang, X. L.; Zhang, J. Z.; He, Y. K.; Zhang, Y. C.; Zhu, W. W. Research on the critical value of prediction indicators in deep coal seams. *J. Petrol Sci.* **2019**, *179*, 868−884.

(2) Yuan, A. Y.; Hu, H.; Yuan, Q. P. A Study of the Laws of Abnormal Gas Emissions and the Stability Controls for Coal Mine Walls in Deeply Buried High-Gas Coal Seams. *Adv. Civ. Eng.* **2020**, *12*, No. 8894854.

(3) Tang, X.; Nino, R. High pressure supercritical carbon dioxide adsorption in coal: Adsorption model and thermodynamic characteristics. *J. CO_2 Util.* **2017**, *18*, 189−197.

(4) Hu, Y. B.; Li, W. P.; Wang, Q. Q.; Liu, S. L.; Wang, Z. K. Study on failure depth of coal seam floor in deep mining. *Environ. Earth Sci.* **2019**, *78*, 697.

(5) Gao, Z.; Li, B. B.; Li, J. H.; Zhang, Y.; Ren, C. H.; Wang, B. Study on the Adsorption and Thermodynamic Characteristics of Methane under High Temperature and Pressure. *Energy Fuels* **2020**, *34*, 15878−15893.

(6) Boon, J.; Cobden, P. D.; van Dijk, H. A. J.; Hoogland, C.; van Selow, E. R.; van Sint, M. Isotherm model for high-temperature, high-pressure adsorption of CO_2 and H_2O on K-promoted hydrotalcite. *Chem. Eng. J.* **2014**, *248*, 406−414.

(7) Qing, H.; Deng, C. B.; Jin, Z. X.; Cao, T. Molecular Simulation of the Adsorption Characteristics of Methane in Pores of Coal with Different Metamorphic Degrees. *Molecules* **2021**, *26*, 7217.

(8) Li, A.; Ding, X. S.; Yu, Z. Z.; Wang, M.; Mu, Q.; Dai, Z. H.; Li, H. Y.; Zhang, B.; Han, T. R. Prediction model of fracture depth and water inrush risk zoning in deep mining coal seam floor. *Environ. Earth Sci.* **2022**, *81*, 315.

(9) Levy, J. H.; Day, S. J.; Killingley, J. S. Methane capacities of Bowen Basin coals related to coal properties. *Fuel* **1997**, *76*, 813−819.

(10) Bustin, R. M.; Clarkson, C. R. Geological controls on coalbed methane reservoir capacity and gas content. *Int. J. Coal Geol.* **1998**, *38*, 3−26.

(11) Sakurovs, R.; Day, S.; Weir, S. Temperature dependence of sorption of gases by coals and charcoals. *Int. J. Coal Geol.* **2007**, *73*, 250−258.

(12) Long, W.; Zhaofeng, W.; Chenjun, Q.; Shujun, M. A.; Jiwei, Y. Physical Simulation of Temperature and Pressure Evolvement in Coal by Different Refrigeration Modes for Freezing Coring. *ACS Omega* **2019**, *4*, 20178−20187.

(13) Liu, G. F.; Zhang, Z. X.; Zhang, X. D. Pore distribution regularity and adsorption-desorption characteristics of gas-fertilized coal and coking coal. *Chin. J. Rock Mech. Eng.* **2009**, *28*, 1587−1592.

(14) Zhang, X. D.; Sang, S. X.; Qin, Y.; Zhang, J.; Tang, J. X. Study on adsorption isotherm of coal samples with different particle sizes. *J. China Univ. Min. Techno.* **2005**, 427−432.

(15) Hong, L.; Gao, D. M.; Wang, J. R.; Zheng, D. Adsorption simulation of open-ended single-walled carbon nanotubes for various gases. *Aip Adv.* **2020**, No. 015338.

(16) Han, W. C.; Li, A. F.; Fang, Q. Comparative analysis of supercritical adsorption isothermal adsorption models for water-bearing coals and rocks. *J. China Coal Soc.* **2020**, *45*, 4095−4103.

(17) Pan, J. N.; Hou, Q. L.; Ju, J. W.; Bai, H. L.; Zhao, Y. Q. Coalbed methane sorption related to coal deformation structures at different temperatures and pressures. *Fuel* **2012**, *102*, 760−765.

(18) Divó-Matos, Y. E.; Cruz-Rodríguez, R. C.; Reguera, L.; Reguera, E. A new model for gas adsorption isotherm at high pressures. *Int. J. Hydrogen Energy* **2021**, *46*, 6613−6622.

(19) Xie, J.; Liang, Y. P.; Zou, Q. L.; Wang, Z. H.; Li, X. L. Prediction Model for Isothermal Adsorption Curves Based on Adsorption Potential Theory and Adsorption Behaviors of Methane on Granular Coal. *Energy Fuels* **2019**, *33*, 1910−1921.

(20) Lu, G. W.; Wei, C. T.; Wang, J. L.; Yan, G. Y.; Zhang, J. J.; Yu, S. Methane Adsorption Characteristics and Adsorption Model Applicability of Tectonically Deformed Coals in the Huaibei Coalfield. *Energy Fuels* **2018**, *32*, 7485−7496.

(21) Deng, J. C.; Kang, J. H.; Zhou, F. B.; Li, H. J.; Zhang, D.; Li, G. H. The adsorption heat of methane on coal: Comparison of theoretical and calorimetric heat and model of heat flow by microcalorimeter. *Fuel* **2019**, *237*, 81−90.

(22) Hou, C.; Zhang, Y. H.; Zhu, C. J. Study on the change of gas adsorption force on the coal bulk surface under high temperature and high pressure. *Saf. Coal Mines* **2019**, *50*, 1−5.

(23) Zhong, R. Q.; Li, S. C.; Yin, F. F.; Nie, B. S. Molecular Model Construction and Study of Gas Adsorption of Zhaozhuang Coal-Junqing Meng. *Energy Fuels* **2018**, *32*, 9727−9737.

(24) Liu, H. H.; Lin, B. Q.; Mou, J. H.; Wei, Y. Experimental study and modelling of coal stress induced by gas adsorption. *J. Nat. Gas Sci. Eng.* **2020**, *74*, 1875−5100.

(25) Xiang, J. H.; Zeng, F. U.; Liang, H. Z.; Li, B.; Song, X. X. Molecular simulation of adsorption of CH_4, CO_2, H_2O in the molecular structure of coal. *Sci. China Earth Sci.* **2014**, *44*, 1418−1428.

(26) Hu, H. X.; Li, X. C.; Fang, Z. M.; Wei, N. Small-molecule gas sorption and diffusion in coal: Molecular simulation. *Energy* **2010**, *35*, 2939−2944.

(27) Khaddour, F.; Knorst-Fouran, A.; Plantier, F.; Pineiro, M. M.; Mendiboure, B.; Miqueu, C. A fully consistent experimental and molecular simulation study of methane adsorption on activated carbon. *Adsorption* **2014**, *20*, 649−656.

(28) Song, Y.; Zhu, Y. M.; Li, M. Macro molecule simulation and CH_4 adsorption mechanism of coal vitrinite. *Appl. Surf. Sci.* **2017**, *396*, 291−302.

(29) Wang, T. Leakage plugging technology of drilling fluid for ″L″ type horizontal well of coalbed methane in Liulin, Shanxi. *Coal Geo China* **2020**, *32*, 163−166.

(30) Huang, J. Y. Application of comprehensive exploration technology in goaf of Pingdingshan Coal Mine. *Coal Technol.* **2013**, *32*, 13−114.

(31) Fan, Z. H.Macromolecular modeling and adsorption mechanism of different rank coals. *China Univ. Geo*, Master's Thesis, **2020**.

(32) Wang, Z. Y.Microstructure evolution of tectonic coal and its influence on gas adsorption and desorption kinetics. *China Min. Technol.*, Master's Thesis, **2020**.

(33) Yan, H. W.; Nie, B. S.; Peng, C. Molecular Model Construction of Low-Quality Coal and Molecular Simulation of Chemical Bond Energy Combined with Materials Studio. *Energy Fuels* **2021**, *35*, 17602−17616.

(34) Meng, J. Q.; Li, S. C.; Niu, J. X.; Meng, H. X.; Zhong, R. Q.; Zhang, L. F.; Nie, B. S. Effects of moisture on methane desorption characteristics of the Zhaozhuang coal: experiment and molecular simulation. *Environ. Earth Sci.* **2020**, *79*, 44.
(35) Qing, H.; Deng, C. B.; Tao, C.; Jin, Z. X. Molecular Simulation on Competitive Adsorption Differences of Gas with Different Pore Sizes in Coal. *Molecules* **2022**, *27*, 1594.
(36) Zhu, H. Q.; Guo, S.; Xie, Y. Y.; Zhao, H. R. Molecular simulation and experimental studies on CO2 and N2 adsorption to bituminous coal. *Environ. Sci. Pollute R.* **2022**, *50*, 127−136.
(37) Li, Y.; Yang, Z. Z.; Li, X. G. Molecular Simulation Study on the Effect of Coal Rank and Moisture on CO_2/CH_4 Competitive Adsorption. *Energy Fuels* **2019**, *33*, 9087−9098.
(38) Cui, X.; Yan, H.; Zhao, P. T. A review of coal molecular structure model construction and analysis methods. *J. China Univ. Min. Technol.* **2019**, *48*, 704−717.
(39) Lv, Z. L.; Ning, Z. F.; Wang, Q.; Meng, H.; Yu, X. F.; Hui, B. Molecular simulation of methane adsorption in shale clay minerals. *J. China Coal Soc.* **2019**, *44*, 3117−3124.
(40) Xiong, J.; Liu, X. J.; Liang, L. X. Molecular Simulation of Methane Adsorption in Clay Mineral Slit Pores. *J. China Coal Soc.* **2017**, *42*, 959−968.
(41) Zhou, J. P.; Xian, X. F.; Li, X. H.; Jiang, D. Y.; Jiang, Y. D. Molecular simulation of competitive adsorption of CO_2 and CH_4 in slit pores. *J. China Coal Soc.* **2010**, *35*, 1512−1517.
(42) Liu, D. M.; Yao, Y. B.; Chang, Y. H. Measurement of adsorption phase densities with respect to different pressure: Potential application for determination of free and adsorbed methane in coalbed methane reservoir. *Chem. Eng. J.* **2022**, No. 137103.
(43) Zhang, M. J.; Yang, M. X.; Jia, T. R. Kinetic characteristics of methane adsorption in supercritical state of anthracite coal from Longshan Mine. *Nat. Gas Geo. Sci.* **2022**, *33*, 267−276.
(44) Liao, Z. W.; Liu, X. F.; Song, D. Z.; He, X. Q.; Nie, B. S.; Yang, T.; Wang, L. K. Micro-structural Damage to Coal Induced by Liquid CO2 Phase Change Fracturing. *Nat. Resour. Res.* **2021**, *30*, 1613−1627.
(45) Xue, P.; Zhang, L. X.; Liang, Q. S.; Shi, Y.; Cao, C. Thermodynamic characteristics of shale adsorption of supercritical CH_4. *Nat. Gas Geo Sci.* **2020**, *31*, 1261−1270.
(46) Li, S. G.; Bai, Y.; Lin, H. F.; Yan, M.; Long, H. Molecular simulation of adsorption thermodynamic properties of CH_4, CO2 and N2 multicomponent gases in coal molecules. *J. China Coal Soc.* **2018**, *43*, 2476−2483.
(47) Zhang, M. J.; Gong, Z.; Tan, Z. H.; Liu, H.; Yang, M. X. Experiment and thermodynamic analysis of coal adsorption of methane based on gravimetric method. *Nat. Gas Geosci.* **2021**, *32*, 589−597.
(48) Zhang, Q. H.; Liu, X. F.; Nie, B. S.; Wu, W. B.; Wang, R. Methane sorption behavior on tectonic coal under the influence of moisture. *Fuel* **2022**, No. 125150.
(49) Ren, W. X.; Li, G. S.; Tian, S. C.; Sheng, M.; Geng, L. D. Adsorption and Surface Diffusion of Supercritical Methane in Shale. *Ind. Eng. Chem. Res.* **2017**, *56*, 3446−3455.
(50) Zhou, S. W.; Xue, H. Q.; Ning, Y.; Guo, W.; Zhang, Q. Experimental study of supercritical methane adsorption in Longmaxi shale: Insights into the density of adsorbed methane. *Fuel.* **2018**, *211*, 140−148.
(51) Liang, C. Y.; Zheng, Q.; Jiang, J. Y.; Monteiro, P. J. M.; Li, F. S. Calcium silicate hydrate colloid at different humidities: Micro-structure, deformation mechanism, and mechanical properties. *Acta Mater.* **2022**, *228*, No. 117740.
(52) Chen, K.; Liu, X. F.; Nie, B. S.; Zhang, C. P.; Song, D. Z.; Wang, L. K.; Yang, T. Mineral dissolution and pore alteration of coal induced by interactions with supercritical CO2. *Energy* **2022**, *248*, No. 123627.
(53) Zhang, J. F.; Jiang, F. X.; Yang, J. B.; Bai, W. S.; Zhang, L. Rockburst mechanism in soft coal seam within deep coal mines. *Int. J. Min. Sci. Technol.* **2022**, *3*, 551−556.

https://doi.org/10.1021/acsomega.2c06593
ACS Omega 2023, 8, 3129−3147